

Inclusive $\bar{B} \rightarrow X_s \ell^+ \ell^-$ with a hadronic mass cut

Tobias Huber¹, Tobias Hurth², Jack Jenkins³, Enrico Lunghi³

¹*Theoretische Physik 1, Center for Particle Physics Siegen (CPPS), Universität Siegen, Walter-Flex-Straße 3, D-57068 Siegen, Germany*

²*PRISMA+ Cluster of Excellence and Institute for Physics (THEP), Johannes Gutenberg University, D-55099 Mainz, Germany*

³*Physics Department, Indiana University, Bloomington, IN 47405, USA*

E-mail: huber@physik.uni-siegen.de, tobias.hurth@cern.ch, jackjenk@iu.edu, elunghi@indiana.edu

ABSTRACT: The hadronic mass spectrum of inclusive $\bar{B} \rightarrow X_s \ell^+ \ell^-$ is investigated at next to leading order in the heavy quark expansion. For mild cuts on the hadronic mass, the expansion, which applies when the cut is released, remains convergent. However, the cuts used at BaBar and Belle to reduce backgrounds from charged current semileptonic processes are too severe for a description in terms of matrix elements of local operators to apply. Strategies for interpolating between the two regions are discussed.

KEYWORDS: Bottom Quarks, Rare Decays, Semi-Leptonic Decays

Contents

1	Introduction	1
2	Theoretical framework	4
2.1	Kinematics	4
2.2	Angular decomposition	4
2.3	Hadronic tensor and form factors	6
3	Results	7
4	Conclusions	14
A	Analytical results	15
A.1	Integrals	15
A.2	Form factors	16
A.2.1	$O(\lambda_1/m_b^2)$	16
A.2.2	$O(\alpha_s)$	17
A.2.3	$O(\alpha_s\lambda_1/m_b^2)$	17
A.3	Hadronic tensors	21
B	Plus distribution technology	23

1 Introduction

The inclusive rare decay $\bar{B} \rightarrow X_s \ell^+ \ell^-$ ($\ell = e, \mu$) proceeds through a flavor changing neutral current (FCNC), which is forbidden in the Born approximation of the Standard Model (SM). However, the underlying $b \rightarrow s$ transition occurs at higher order through simultaneous emission of a pair of charged gauge bosons, or emission of a neutral gauge boson from a virtual charged gauge boson or quark. Therefore $\bar{B} \rightarrow X_s \ell^+ \ell^-$ directly probes the quantum fluctuations of the SM at the electroweak scale, and is sensitive to potential physics beyond the SM [1, 2].

Tensions between measurements and SM predictions in precision B physics, known as the B anomalies, have persisted over the last decade, mainly driven by LHCb results on branching fractions and angular observables of exclusive modes with muons such as $\bar{B} \rightarrow K \mu^+ \mu^-$ and $\bar{B} \rightarrow K^* \mu^+ \mu^-$ [3–12]. Such observables suffer from power corrections which are difficult to access, among them hadronic contributions from virtual charm quarks which are not described within QCD factorization. While these nonlocal matrix elements can be addressed with analyticity methods [13], it is currently not possible to confidently separate new physics (NP) from them; the NP significance of the tensions presently depends on order of magnitude estimates for these unknown long distance effects [14, 15].

On the other hand, the ratios R_K and R_{K^*} of branching fractions into muons compared to electrons are theoretically very clean, with uncertainties of less than one percent and central values close to unity in the SM due to lepton flavor universality [16]. Tensions in R_K and R_{K^*} were reported at the level of 3σ by LHCb [17, 18]. The crucial issue in this context is that the tensions were rather consistent with the previously found tensions in the angular observables; the persistence of the tensions in R_K and R_{K^*} supported the NP interpretation in the other exclusive observables, despite their sensitivity to long distance physics [19]. However, the anomaly has evaporated in the latest LHCb measurement [20] which is now one of the most precise measurements in FCNC transitions, and along with it, the option to disentangle NP in the exclusive modes with a clean observable.

Since R_K and R_{K^*} are now consistent with the SM, investigating the inclusive mode $\bar{B} \rightarrow X_s \mu^+ \mu^-$ is the only remaining option to resolve the persisting anomalies in the exclusive modes such as $\bar{B} \rightarrow K \mu^+ \mu^-$ and $\bar{B} \rightarrow K^* \mu^+ \mu^-$. Inclusive and exclusive decays offer complementary information in the search for NP in $b \rightarrow s$ transitions [21]. However, inclusive decays are much cleaner, as they are analyzed in the operator product expansion (OPE) in terms of a handful of local matrix elements, and bounds on nonlocal power corrections originating from resolved virtual photons can be calculated within Soft Collinear Effective Theory (SCET) [22–24].

In the future the inclusive mode will be measured at Belle II with high precision [25]. A semi-inclusive measurement might be possible even at LHCb [26]. Presently, inclusive measurements are available from BaBar [27, 28] and Belle [29, 30] with combined statistics on electrons and muons. The results¹

$$\mathcal{B}[1, 6]_{\ell\ell}^{\text{exp}} = \begin{cases} (1.49 \pm 0.50_{-0.32}^{+0.41}) \times 10^{-6} & \text{Belle} \\ (1.60_{-0.39-0.13}^{+0.41+0.17} \pm 0.18) \times 10^{-6} & \text{BaBar} \end{cases} \quad (1.1)$$

are compatible with each other and with the SM predictions [21]

$$\mathcal{B}[1, 6]_{ee}^{\text{SM}} = (1.78 \pm 0.13) \times 10^{-6}, \quad \mathcal{B}[1, 6]_{\mu\mu}^{\text{SM}} = (1.73 \pm 0.13) \times 10^{-6}. \quad (1.2)$$

The first two uncertainties indicated in eq. (1.1) are statistical and systematic, respectively. The final uncertainty on the BaBar result accounts, separately from other systematics, the reconstruction of missing modes using a sum-over-exclusive tagging method. The missing modes include modes removed by a cut $M_X < 1.8 \text{ GeV}$ (for Belle $M_X < 2.0 \text{ GeV}$) necessary to reduce double semileptonic backgrounds from same and/or opposite side decays $\bar{B} \rightarrow X_c(\rightarrow X \ell^+ \nu) \ell^- \nu$ and $\bar{B}(\rightarrow X_c \ell^- \nu) B(\rightarrow X_c \ell^+ \nu)$ respectively. With sufficient statistics at Belle II, it may be feasible to use the recoil tagging method, in which the kinematics of the X_s system is determined indirectly by tagging the fully hadronic decays of the partner B meson and the lepton momenta in $\bar{B} \rightarrow X \ell^+ \ell^-$. However, a cut on the hadronic mass will probably still be necessary to reduce backgrounds from $\bar{B} \rightarrow X_c(\rightarrow X \ell^+ \nu) \ell^- \nu$ on the signal side.

At BaBar and Belle, the effect of the cut on the hadronic invariant mass was taken into account with a signal Monte Carlo formed by smearing the spectrum of $b \rightarrow s(g) \ell^+ \ell^-$

¹ $[q_1^2, q_2^2]$ indicates the bin $q_1^2 < m_{\ell\ell}^2 < q_2^2$ in units of GeV^2 .

with a Gaussian Fermi motion model [31]. Alternatively, measurements of $\bar{B} \rightarrow X_s \ell^+ \ell^-$ with a hadronic mass cut can be compared to the corresponding theory predictions, using the framework of SCET to address the multi-scale problem introduced by the hadronic mass cut. At leading order in $1/m_b$, there is a single shape function which is universal to all heavy-to-light-current B decays [32, 33]. These shape functions represent the soft functions in the factorization within SCET and are well-defined HQET (Heavy Quark Effective Theory) matrix elements. The effect of the hadronic mass cut was first analyzed in [34], but with some simplifications and certain problems about the SCET scaling of the virtual photon in the low dilepton-mass region as indicated in [22, 23, 35]. At order $1/m_b$, five subleading shape functions appear, and enter with different kernels in SCET convolution integrals for various heavy-to-light decays. The uncertainty due to these subleading shape functions is presently estimated at 5 – 10% [34, 36]. It might be possible to reduce this uncertainty by incorporating more information on moments of the subleading shape functions within HQET (see e.g. [37]).

In this article we follow another strategy to reduce the uncertainty due to the hadronic mass cut. We consider the effect of the hadronic mass cut for mild cuts in the OPE region and analyze the validity of the OPE by studying the explosion of power corrections as the cut is lowered into the shape function region ($M_X^{\text{cut}} \sim \sqrt{\Lambda m_b}$). Since the OPE region does not overlap with the cuts in the shape function region required by experiment, in the future, as a next step an interpolation between the OPE region and the shape function region using SCET is planned. Ratios of observables with the same hadronic mass cut are suitable for investigating the interpolation. Certain $\bar{B} \rightarrow X_s \ell^+ \ell^-$ observables are already known to be independent of the shape function in SCET at least at leading order in $1/m_b$, such as the zero-crossing of the forward-backward asymmetry [35].

For this purpose, we compute the fully differential distribution of $\bar{B} \rightarrow X_s \ell^+ \ell^-$ at $O(\alpha_s)$ in the OPE. We also compute those power corrections at $O(\alpha_s/m_b^2)$ which are the most divergent in $1/M_X^{\text{cut}}$ and use them as an indicator for the breakdown of the OPE. Moreover, the three $\bar{B} \rightarrow X_s \ell^+ \ell^-$ angular observables, together with the $\bar{B} \rightarrow X_u \ell^- \nu$ branching fraction, all with the same hadronic mass cut, constitute a basis of four heavy-to-light-current observables from which three normalized observables, which are both sensitive to NP and rather independent of the hadronic mass cut, can be constructed. We anticipate that both perturbative and nonperturbative corrections are essentially eliminated in these ratios in the OPE region.

The organization of this paper is as follows. In section 2, the effective Lagrangian and angular decomposition of $\bar{B} \rightarrow X_s \ell^+ \ell^-$ is reviewed. In section 3, results for the effect of the hadronic mass cut on the rate and angular observables of $\bar{B} \rightarrow X_s \ell^+ \ell^-$ are presented. We summarize in section 4 and relegate technical details to appendices A and B.

2 Theoretical framework

Integrating out electroweak gauge bosons, the top quark and Higgs boson from the SM leads to an effective Lagrangian

$$\mathcal{L}(b \rightarrow s \ell^+ \ell^-) = \frac{4G_F}{\sqrt{2}} V_{ts}^* V_{tb} \sum_{i=1}^{10} C_i Q_i, \quad (2.1)$$

where $Q_{3\dots 6}$ are QCD penguin operators and

$$Q_1 = (\bar{s}\gamma_\mu P_L T^a c)(\bar{c}\gamma^\mu P_L T^a b), \quad Q_2 = (\bar{s}\gamma_\mu P_L c)(\bar{c}\gamma^\mu P_L b), \quad (2.2)$$

$$Q_7 = \frac{em_b}{16\pi^2} (\bar{s}\sigma^{\mu\nu} P_R b) F_{\mu\nu}, \quad Q_8 = \frac{gm_b}{16\pi^2} (\bar{s}\sigma^{\mu\nu} P_R T^a b) G_{\mu\nu}^a,$$

$$Q_9 = \frac{\alpha}{4\pi} (\bar{s}\gamma_\mu P_L b)(\bar{\ell}\gamma^\mu \ell), \quad Q_{10} = \frac{\alpha}{4\pi} (\bar{s}\gamma_\mu P_L b)(\bar{\ell}\gamma^\mu \gamma_5 \ell). \quad (2.3)$$

To arrive at eq. (2.1) we used CKM unitarity and neglected $V_{us}^* V_{ub} = O(\lambda^4)$ compared to $V_{ts}^* V_{tb} = O(\lambda^2)$ with the Wolfenstein parameter $\lambda \sim 0.22$, which is appropriate for the purposes of the present article.

2.1 Kinematics

The fully differential $\bar{B} \rightarrow X_s \ell^+ \ell^-$ rate is defined by three kinematical invariants, such as the dilepton mass square $q^2 = (p_{\ell^+} + p_{\ell^-})^2$, the dilepton energy $v \cdot q$, where $v = p_B/M_B$ is the heavy meson velocity which satisfies $v^2 = 1$, and an angular variable $z = \cos \theta$, where θ is the angle between the positively charged lepton momentum and the B meson momentum in the dilepton center of momentum frame,

$$z = \frac{v \cdot (p_{\ell^-} - p_{\ell^+})}{\sqrt{(v \cdot q)^2 - q^2}}. \quad (2.4)$$

We also define

$$s = \frac{q^2}{m_b^2}, \quad u = \frac{(m_b v - q)^2}{m_b^2}, \quad (2.5)$$

which appear in the calculation of the partonic decay process $b \rightarrow s(g)\ell^+\ell^-$, in particular in the combinations (using similar notation as [38])

$$w = 1 - s, \quad \lambda = (w + u)^2 - 4u, \quad \mathcal{I} = \frac{1}{\sqrt{\lambda}} \ln \frac{w + u + \sqrt{\lambda}}{w + u - \sqrt{\lambda}}. \quad (2.6)$$

2.2 Angular decomposition

The branching fraction of $\bar{B} \rightarrow X_s \ell^+ \ell^-$ is quadratic in the angular variable z at leading order in QED and can be decomposed into three angular observables [39],

$$\frac{d^3\mathcal{B}}{ds du dz} = \frac{3}{8} \left[(1 + z^2) \frac{d^2\mathcal{H}_T}{ds du} + 2z \frac{d^2\mathcal{H}_A}{ds du} + 2(1 - z^2) \frac{d^2\mathcal{H}_L}{ds du} \right] + O(\alpha_e). \quad (2.7)$$

For the definitions of the angular observables in the presence of QED corrections, see [40]. In the following, we work at lowest order in QED. The double differential branching fraction is given by

$$\frac{d^2\mathcal{B}}{ds du} = \frac{d^2\mathcal{H}_L}{ds du} + \frac{d^2\mathcal{H}_T}{ds du}. \quad (2.8)$$

The angular observables depend on the Wilson coefficients according to²

$$\begin{aligned} \frac{d^2\mathcal{H}_T}{ds du} = & 2\Gamma_0(1-s)^2 s \left[(|C_9^{\text{eff}}|^2 + C_{10}^2) h_T^{99}(s, u) + \frac{4}{s^2} |C_7^{\text{eff}}|^2 h_T^{77}(s, u) \right. \\ & \left. + \frac{4}{s} \text{Re}(C_7^{\text{eff}*} C_9^{\text{eff}}) h_T^{79}(s, u) \right] + \frac{d^2\mathcal{H}_T^{\text{brems}}}{ds du}, \end{aligned} \quad (2.9)$$

$$\begin{aligned} \frac{d^2\mathcal{H}_A}{ds du} = & -4\Gamma_0(1-s)^2 s \left[\text{Re}(C_9^{\text{eff}}) C_{10} h_A^{90}(s, u) + \frac{2}{s} \text{Re}(C_7^{\text{eff}}) C_{10} h_A^{70}(s, u) \right] \\ & + \frac{d^2\mathcal{H}_A^{\text{brems}}}{ds du}, \end{aligned} \quad (2.10)$$

$$\begin{aligned} \frac{d^2\mathcal{H}_L}{ds du} = & \Gamma_0(1-s)^2 \left[(|C_9^{\text{eff}}|^2 + C_{10}^2) h_L^{99}(s, u) + 4|C_7^{\text{eff}}|^2 h_L^{77}(s, u) \right. \\ & \left. + 4\text{Re}(C_7^{\text{eff}*} C_9^{\text{eff}}) h_L^{79}(s, u) \right] + \frac{d^2\mathcal{H}_L^{\text{brems}}}{ds du}, \end{aligned} \quad (2.11)$$

where

$$\Gamma_0 = \frac{G_F^2 m_b^5}{48\pi^3 \tau_B} |V_{tb}^* V_{ts}|^2. \quad (2.12)$$

At tree level, the form factors are given by $h_I^{ij}(s, u) = \delta(u)$, so the q^2 dependence of the contribution of each product of coefficients to each observable can be understood by setting the form factors to unity. The effective coefficients $C_{7,9}^{\text{eff}}$ absorb into $C_{7,9}$ the matrix elements of other operators in the effective theory which are proportional to the tree level matrix element of $Q_{7,9}$. Including the α_s corrections to the Wilson coefficients would modify the hadronic mass spectrum at a higher order α_s^2 . Such matrix elements in the case of C_7 are order α_s and not included.

$$C_7^{\text{eff}}(s) = C_7^{(11)}(\mu_b), \quad (2.13)$$

$$C_9^{\text{eff}}(s) = C_9^{(11)}(\mu_b) + \frac{4\pi}{\alpha_s(\mu_b)} C_9^{(01)}(\mu_b) + \left(\frac{4}{3} C_1^{(00)} + C_2^{(00)} \right) f_2(s). \quad (2.14)$$

The coefficients $C_i^{(nm)}$ of the $\alpha_s^n \kappa^m$ term of the double expansion in α_s and $\kappa = \alpha_e/\alpha_s$ were calculated in [41]. Below the charm pair production threshold, the loop function $f(s)$ is real, and is given by

$$f_2(s) = \frac{4}{9} \left[\ln \frac{\mu_b^2}{m_c^2} + \frac{2}{3} + \zeta - (2 + \zeta) \sqrt{\zeta - 1} \arctan \frac{1}{\sqrt{\zeta - 1}} \right], \quad \zeta = \frac{4m_c^2}{q^2}. \quad (2.15)$$

²Interference terms involving the operator Q_{10} are designated by the superscript 0

Finally, the bremsstrahlung terms in eqs. (2.9) – (2.11) refer to the matrix elements of other operators in the effective theory which are not proportional to the tree level matrix elements of $Q_{7,9,10}$.

We also define the normalized forward backward asymmetry \bar{A}_{FB} and fraction of transverse polarization F_T according to

$$\bar{A}_{\text{FB}} = \frac{3}{4} \frac{\mathcal{H}_A}{\mathcal{H}_T + \mathcal{H}_L}, \quad F_T = \frac{\mathcal{H}_T}{\mathcal{H}_T + \mathcal{H}_L}. \quad (2.16)$$

Both fractions are suppressed in the low- q^2 region due to the prefactor s in eq. (2.9) for \mathcal{H}_T and eq. (2.10) for \mathcal{H}_A , which does not appear in eq. (2.11) for \mathcal{H}_L . Moreover, the two Wilson coefficients in the combination $C_9 + 2C_7/s$ appearing in eq. (2.10) approximately cancel in the low- q^2 region, suppressing the forward backward asymmetry. The fraction F_T is also suppressed since \mathcal{H}_T depends on C_9 through the combination $|C_9 + 2C_7/s|^2$.

2.3 Hadronic tensor and form factors

Having outlined the main ingredients in the phenomenology of $\bar{B} \rightarrow X_s \ell^+ \ell^-$, the starting point of a formal treatment of inclusive semileptonic decays in QCD is an analysis of the hadronic tensor, which is defined by the matrix element of the time ordered product of currents in QCD,

$$W_{\mu\nu}^{ij}(v, q) = -\frac{1}{\pi} \text{Im} \left[-i \int d^4x e^{-iqx} \frac{\langle \bar{B}(v) | T J_\mu^{\dagger i}(x) J_\nu^j(0) | \bar{B}(v) \rangle}{2M_B} \right]. \quad (2.17)$$

The semileptonic and radiative currents are

$$J_\mu^9 = J_\mu^{10} = \bar{s} \gamma_\mu P_L b, \quad J_\mu^7 = -\frac{2m_b}{q^2} (\bar{s} i \sigma_{\mu\nu} P_R b) q^\nu. \quad (2.18)$$

Note that the hadronic currents for the operators Q_9 and Q_{10} are identical. Therefore $W_{\mu\nu}^{99} = W_{\mu\nu}^{90} = W_{\mu\nu}^{00}$ and $W_{\mu\nu}^{79} = W_{\mu\nu}^{70}$. The hadronic tensor is a function of v and q , and can be decomposed into five form factors

$$W_{\mu\nu}^{ij}(v, q) = -g_{\mu\nu} W_1^{ij}(q^2, v \cdot q) + v_\mu v_\nu W_2^{ij}(q^2, v \cdot q) + i \epsilon_{\mu\nu\alpha\beta} v^\alpha q^\beta W_3^{ij}(q^2, v \cdot q) + q_\mu q_\nu W_4^{ij}(q^2, v \cdot q) + (v_\mu q_\nu + v_\nu q_\mu) W_5^{ij}(q^2, v \cdot q) \quad (2.19)$$

of which only the first three contribute to $\bar{B} \rightarrow X_s \ell^+ \ell^-$ for massless leptons. At next to leading order (NLO) the hadronic tensor is calculated from diagrams depicted in figure 1. The form factors are related by

$$h_T^{99} = \frac{4\sqrt{\lambda}}{(1-s)^2} W_1^{99}, \quad h_T^{77} = \frac{\sqrt{\lambda} s^2}{(1-s)^2} W_1^{77}, \quad h_T^{79} = \frac{2\sqrt{\lambda} s}{(1-s)^2} W_1^{79}, \quad (2.20)$$

$$h_A^{90} = \frac{2\lambda}{(1-s)^2} W_3^{99}, \quad h_A^{70} = \frac{\lambda s}{(1-s)^2} W_3^{79}, \quad (2.21)$$

$$h_L^{99} = \frac{\sqrt{\lambda}(4sW_1^{99} + \lambda W_2^{99})}{(1-s)^2}, \quad h_L^{77} = \frac{\sqrt{\lambda}(4sW_1^{77} + \lambda W_2^{77})}{4(1-s)^2}, \quad h_L^{79} = \frac{\sqrt{\lambda}(4sW_1^{79} + \lambda W_2^{79})}{2(1-s)^2}. \quad (2.22)$$

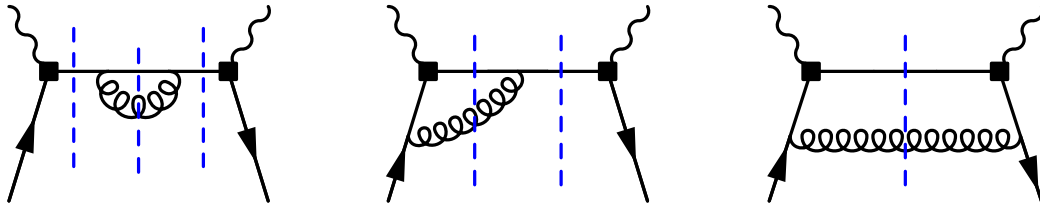


Figure 1: The hadronic tensor at NLO from unitarity cuts. Square vertices are insertions of $Q_{7,9,10}$. Only one of the two vertex corrections is shown.

3 Results

In this section, we present results for the effect of a hadronic mass cut on the process $\bar{B} \rightarrow X_s \ell^+ \ell^-$ at low- q^2 at $O(\alpha_s)$. The SM predictions for $\bar{B} \rightarrow X_s \ell^+ \ell^-$ without a hadronic mass cut were updated recently in [21]. For large values of M_X^{cut} , the form factors can be expanded in local operators

$$h_I^{ij} = \sum_{n=0}^{\infty} \left(\frac{\alpha_s}{4\pi} \right)^n \left[h_I^{ij(n)} + h_I^{ij(\lambda_1, n)} \frac{\lambda_1}{m_b^2} + h_I^{ij(\lambda_2, n)} \frac{\lambda_2}{m_b^2} \right] + O(1/m_b^3), \quad (3.1)$$

where the normalization is such that, at lowest order, $h_I^{ij(0)} = \delta(u)$. The NLO corrections to the partonic decay rate are given by the functions $h_I^{ij(1)}$. Results for these functions are new, and have the form

$$h_I^{ij(1)}(s, u) = -4C_F \left[\frac{\ln u}{u} \right]_+ - C_F (7 - 8 \ln w) \left[\frac{1}{u} \right]_+ + h_{I,\delta}^{ij(1)} \delta(u) + h_{I,\theta}^{ij(1)} \theta(u) \quad (3.2)$$

in terms of distributions in the partonic mass variable u . The coefficients of the plus distributions are universal, i.e. the same for each product of Wilson coefficients to each angular observable. The coefficients of the other distributions depend on the combination of Wilson coefficients which enter each angular observable. They are tabulated in Appendix A.2, and are also provided in electronic form in the supplementary materials.

One subtlety is that the expansion in terms of local operators in eq. (3.1) requires $u \sim 1$. It is curious then, that these results are to be used for phenomenology of $\bar{B} \rightarrow X_s \ell^+ \ell^-$ with a cut $M_X < M_X^{\text{cut}}$ which includes the region $u \ll 1$. However, the integral over the region $u \in [0, U]$ is to be interpreted as the difference of the bins $u \in [0, U_{\text{max}}]$ and $u \in [U, U_{\text{max}}]$, where the first bin is the standard OPE integrated over the full hadronic mass spectrum, which admits a local expansion via analytic continuation to $u < 0$, and the second is assumed to admit an OPE locally in $u \sim 1$. In practice, logarithms appear in the integrals

$$\int_0^U du \left[\frac{1}{u} \right]_+ = \ln U, \quad \int_0^U du \left[\frac{\ln u}{u} \right]_+ = \frac{1}{2} \ln^2 U. \quad (3.3)$$

If the hadronic mass cut is in the OPE region, i.e. $U \sim 1$, these logarithms are not large and do not require resummation. Therefore, each term in eq. (3.2) is of equal importance.

The power corrections $h_I^{ij(\lambda_1, n)}$ are related to the leading power corrections $h_I^{ij(n)}$ order by order in perturbation theory through reparameterization invariance (RPI) relations [42]. We find, at lowest order,

$$h_I^{ij(\lambda_1, 0)} = -\frac{1}{6}w^2\delta''(u) - \frac{1}{2}(2-w)\delta'(u) + h_{I,\delta}^{ij(\lambda_1, 0)}\delta(u) \quad (3.4)$$

and at NLO,

$$\begin{aligned} h_I^{ij(\lambda_1, 1)} &= \frac{4C_F w^2}{3} \left[\frac{\ln u}{u^3} \right]_+ + \frac{C_F w^2}{3} (1 - 8 \ln w) \left[\frac{1}{u^3} \right]_+ \\ &- 2C_F (2-w) \left[\frac{\ln u}{u^2} \right]_+ - \frac{C_F}{6} (2 + 3w - 24(2-w) \ln w) \left[\frac{1}{u^2} \right]_+ \\ &+ h_{I, [\ln/1]_+}^{ij(\lambda_1, 1)} \left[\frac{\ln u}{u} \right]_+ + h_{I, [1]_+}^{ij(\lambda_1, 1)} \left[\frac{1}{u} \right]_+ \\ &+ h_{I, \delta''}^{ij(\lambda_1, 1)} \delta''(u) + h_{I, \delta'}^{ij(\lambda_1, 1)} \delta'(u) + h_{I, \delta}^{ij(\lambda_1, 1)} \delta(u) + h_{I, \theta}^{ij(\lambda_1, 1)} \theta(u). \end{aligned} \quad (3.5)$$

The first two lines of eq. (3.5) are generated exclusively from the derivatives of the plus distributions in eq. (3.2), and are therefore also universal. The second two lines contain pieces from the finite terms of eq. (3.2).

The calculation of the $h_I^{ij(\lambda_2, 1)}$ corrections cannot be carried out using RPI relations, and is not attempted here. The structure of these corrections, however, can be inferred from the recent calculation of the hadronic mass distribution of $\bar{B} \rightarrow X_u \ell^- \nu$ at order α_s/m_b^2 [38]. The highest order plus distributions in $h_{ij}^{I(\lambda_2, 1)}$ are quadratic in $1/u$, rather than cubic as in the first line of eq. (3.5). These quadratic divergences are not universal, as in the second line of eq. (3.5). Schematically, their structure is

$$h_I^{ij(\lambda_2, 0)}(s, u) = h_{I, \delta'}^{ij(\lambda_2, 0)} \delta'(u) + h_{I, \delta}^{ij(\lambda_2, 0)} \delta(u) \quad (3.6)$$

and

$$\begin{aligned} h_I^{ij(\lambda_2, 1)}(s, u) &= h_{I, [\ln/2]_+}^{ij(\lambda_2, 1)} \left[\frac{\ln u}{u^2} \right]_+ + h_{I, [2]_+}^{ij(\lambda_2, 1)} \left[\frac{1}{u^2} \right]_+ \\ &+ h_{I, [\ln/1]_+}^{ij(\lambda_2, 1)} \left[\frac{\ln u}{u} \right]_+ + h_{I, [1]_+}^{ij(\lambda_2, 1)} \left[\frac{1}{u} \right]_+ \\ &+ h_{I, \delta''}^{ij(\lambda_2, 1)} \delta''(u) + h_{I, \delta'}^{ij(\lambda_2, 1)} \delta'(u) + h_{I, \delta}^{ij(\lambda_2, 1)} \delta(u) + h_{I, \theta}^{ij(\lambda_2, 1)} \theta(u). \end{aligned} \quad (3.7)$$

To complete the calculation of the hadronic mass spectrum in the OPE at $O(\alpha_s/m_b^2)$, the coefficient functions in the equations above need to be computed in the future.

The branching fraction of $\bar{B} \rightarrow X_s \ell^+ \ell^-$ integrated in a bin $q_1^2 < q^2 < q_2^2$, with and without a hadronic mass cut $M_X < M_X^{\text{cut}}$, is

$$\mathcal{B}[q_1^2, q_2^2, M_X^{\text{cut}}] = \int_{s_1}^{s_2} ds \int_0^{(1-\sqrt{s})^2} du \theta(M_X^{\text{cut}} - M_X) \frac{d^2 \mathcal{B}}{ds du}, \quad (3.8)$$

$$\mathcal{B}[q_1^2, q_2^2] = \int_{s_1}^{s_2} ds \int_0^{(1-\sqrt{s})^2} du \frac{d^2 \mathcal{B}}{ds du}, \quad (3.9)$$

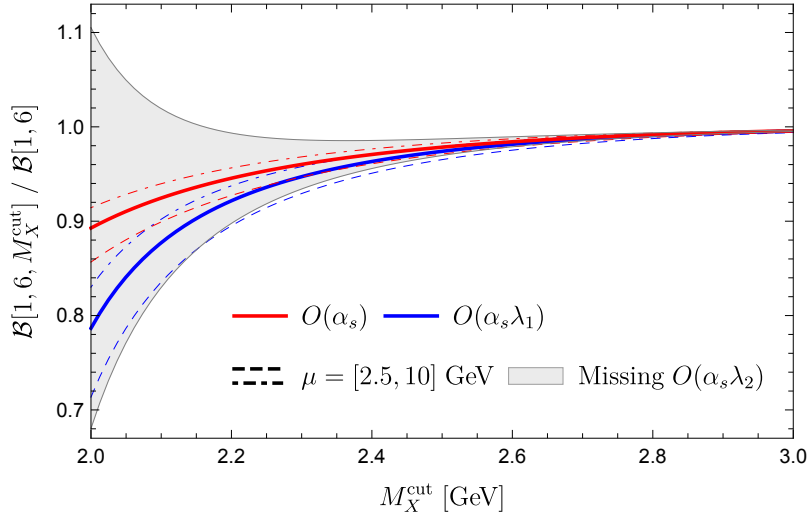


Figure 2: Impact of a cut on the hadronic invariant mass on the low- q^2 branching fraction. Red and blue curves include up to $O(\alpha_s)$ and $O(\alpha_s \lambda_1/m_b^2)$ corrections, respectively. Dashed, solid and dot-dashed lines correspond to $\mu_b = [2.5, 5, 10]$ GeV, respectively. The gray band is a conservative bound on $O(\alpha_s \lambda_2/m_b^2)$ power corrections which are not yet available.

where s, u are defined in eq. (2.5), and

$$M_X = \sqrt{u m_b^2 + m_b (M_B - m_b) (1 - s + u) + (M_B - m_b)^2}. \quad (3.10)$$

The integral kernel in eqs. (3.8) and (3.9) is given via eqs. (2.8), (2.9) and (2.11) in terms of form factors with an expansion in α_s and $1/m_b$ in eq. (3.1). The $O(\alpha_s)$, $O(\lambda_1/m_b^2)$ and $O(\alpha_s \lambda_1/m_b^2)$ terms of this expansion are given in eqs. (3.2), (3.4) and (3.5).

In the ratio $\mathcal{B}[q_1^2, q_2^2, M_X^{\text{cut}}]/\mathcal{B}[q_1^2, q_2^2]$, the common factor in eq. (2.12) cancels. The only inputs that are needed to study the cut dependence are $m_b^{\text{1S}} = 4.691(37)$ GeV and $\lambda_1 = -0.267(90)$ GeV² from [43, 44], $M_B = 5.279$ GeV and $\alpha_s(M_Z) = 0.1179(9)$ from [45] and $m_c^{\text{pole}} = 1.77(14)$ GeV [46], in addition to the Wilson coefficients from [41]. The red curve in figure 2 shows the impact of a hadronic mass cut for $\mathcal{B}[1, 6]$ at $O(\alpha_s)$. The blue curve includes also $O(\lambda_1/m_b^2)$ and $O(\alpha_s \lambda_1/m_b^2)$ corrections. The calculation is not complete at $O(\alpha_s/m_b^2)$ since $O(\alpha_s \lambda_2/m_b^2)$ corrections are not yet available. However, the missing $O(\alpha_s \lambda_2/m_b^2)$ corrections in eq. (3.7) do not contain $1/u^3$ plus distributions which appear for the $O(\alpha_s \lambda_1/m_b^2)$ ones in eq. (3.5). Hence, at low M_X^{cut} , the $O(\alpha_s \lambda_2/m_b^2)$ corrections are expected to be subdominant with respect to the $O(\alpha_s \lambda_1/m_b^2)$ ones. Therefore, the grey band, which is centered on the red curve and has a radius twice the size of the difference between red and blue curves, provides a conservative estimate of the missing power corrections at order $1/m_b^2$.

For $M_X^{\text{cut}} = 2.0$ GeV, the $O(\alpha_s)$ correction decreases the integrated branching fraction by about 10% and the $O(\alpha_s \lambda_1/m_b^2)$ effect is equally large and further lowers the branching fraction by another 10%. It is important to stress that the large impact of the λ_1 correction

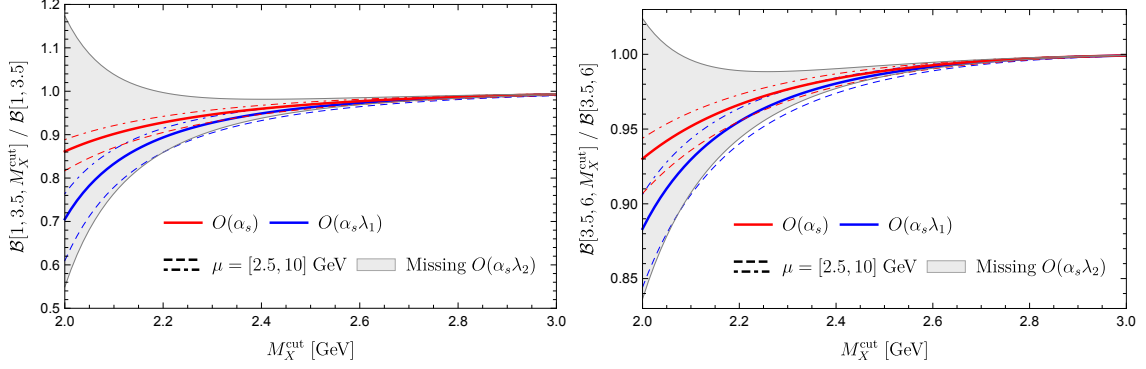


Figure 3: Impact of a cut on the hadronic invariant mass on the low- q^2 branching fraction separated into two bins. See the caption in figure 2 for further details.

at $M_X^{\text{cut}} = 2.0$ GeV signals a breakdown of the OPE: the grey band cannot be interpreted as an estimate of power corrections to all orders in $1/m_b$ there, since their convergence is not guaranteed. A threshold can be tentatively set at $M_X^{\text{cut}} \gtrsim 2.5$ GeV, for which the grey band may be used to estimate the corrections from λ_2 as well as higher order power corrections. The same analysis for the branching fraction separated into two bins in the low- q^2 region is shown in figure 3. The ratios $\mathcal{H}_I[q_1^2, q_2^2, M_X^{\text{cut}}] / \mathcal{H}_I[q_1^2, q_2^2]$ for the angular observables can be built using eqs. (3.8) and (3.9) with $\mathcal{B} \rightarrow \mathcal{H}_I$, and are shown in figure 4. The results presented in figures 2, 3 and 4 are all very similar, and the discussion above for the branching fraction applies to these observables as well.

The qualitative difference between the cuts at 2.0 GeV and 2.5 GeV can be understood by converting from the hadronic mass to the partonic mass $\sqrt{u}m_b$, using eq. (3.10). The partonic mass corresponds to the offshellness of the strange quark in the OPE, and must be larger than the scale $\Lambda \sim 1$ GeV in order for the OPE to make sense. For $M_X^{\text{cut}} = 2.0$ GeV, putting $1 \text{ GeV}^2 < q^2 < 6 \text{ GeV}^2$, the partonic mass cut falls within the range $0.95 \text{ GeV} < \sqrt{u_{\text{cut}}}m_b < 1.21 \text{ GeV}$. For $M_X^{\text{cut}} = 2.5$ GeV, $1.70 \text{ GeV} < \sqrt{u_{\text{cut}}}m_b < 1.86 \text{ GeV}$. The lower endpoint of this range is similar to the mass of the τ lepton, whose inclusive hadronic decays are analyzed with an OPE. Therefore, one may be optimistic that a cut $M_X^{\text{cut}} = 2.5$ GeV is sufficiently high to analyze $\bar{B} \rightarrow X_s \ell^+ \ell^-$ with an OPE as well. Our explicit results at $O(\alpha_s \lambda_1 / m_b^2)$ presented in figures 2, 3 and 4 support this conclusion.

In figure 5 we present our results for the cut dependence of the observables F_T and \bar{A}_{FB} . Due to limited statistics on $\bar{B} \rightarrow X_s \ell^+ \ell^-$, the numerators and denominators of eq. (2.16) will probably need to be binned separately. To be precise,

$$\bar{A}_{\text{FB}}[q_1^2, q_2^2, M_X^{\text{cut}}] = \frac{\int_{s_1}^{s_2} ds \int_0^{(1-\sqrt{s})^2} du \theta(M_X^{\text{cut}} - M_X) \frac{3}{4} \frac{d^2 \mathcal{H}_A}{ds du}}{\int_{s_1}^{s_2} ds \int_0^{(1-\sqrt{s})^2} du \theta(M_X^{\text{cut}} - M_X) \frac{d^2 \mathcal{B}}{ds du}}, \quad (3.11)$$

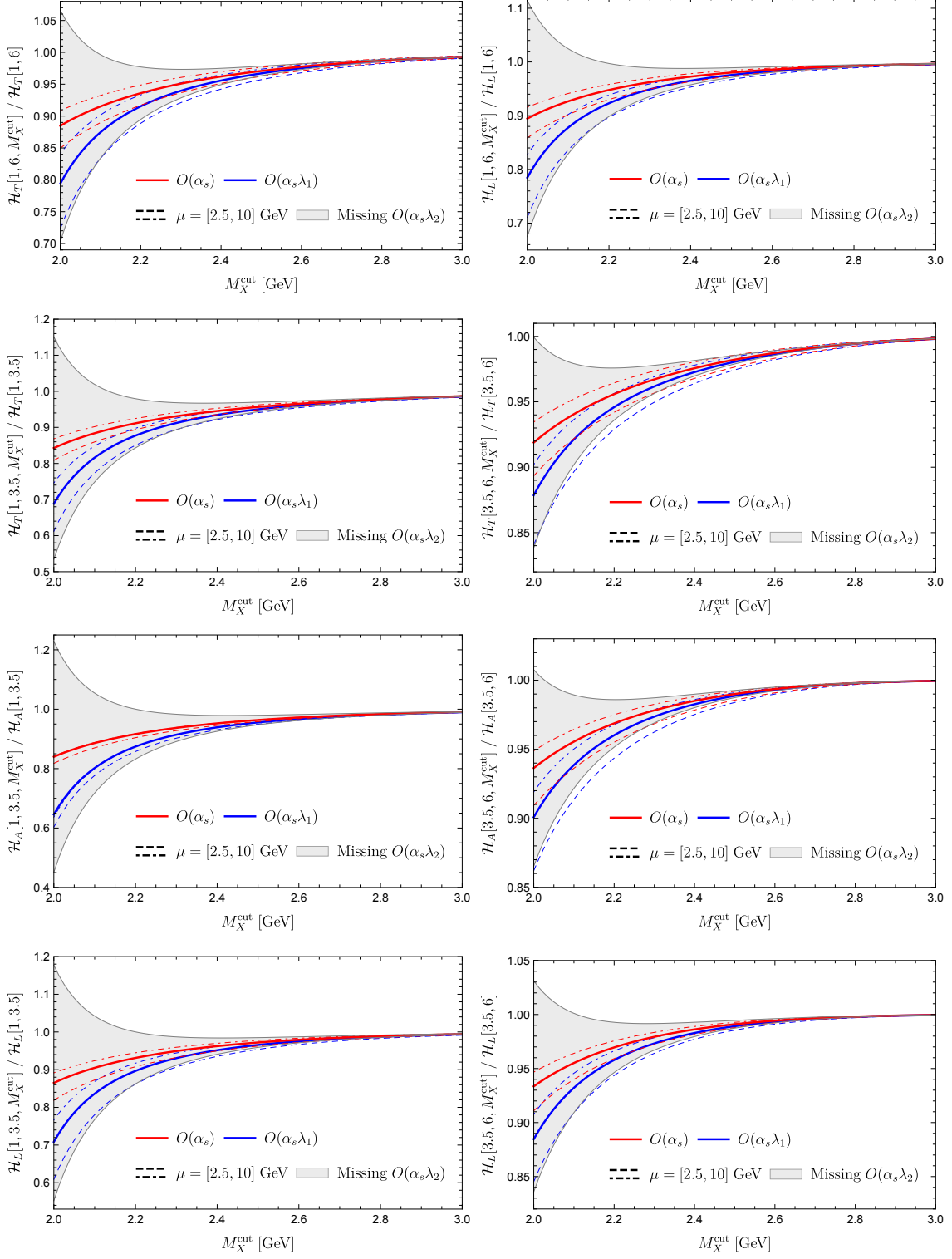


Figure 4: Impact of a cut on the hadronic invariant mass on the low- q^2 angular observables. See the caption in figure 2 for further details.

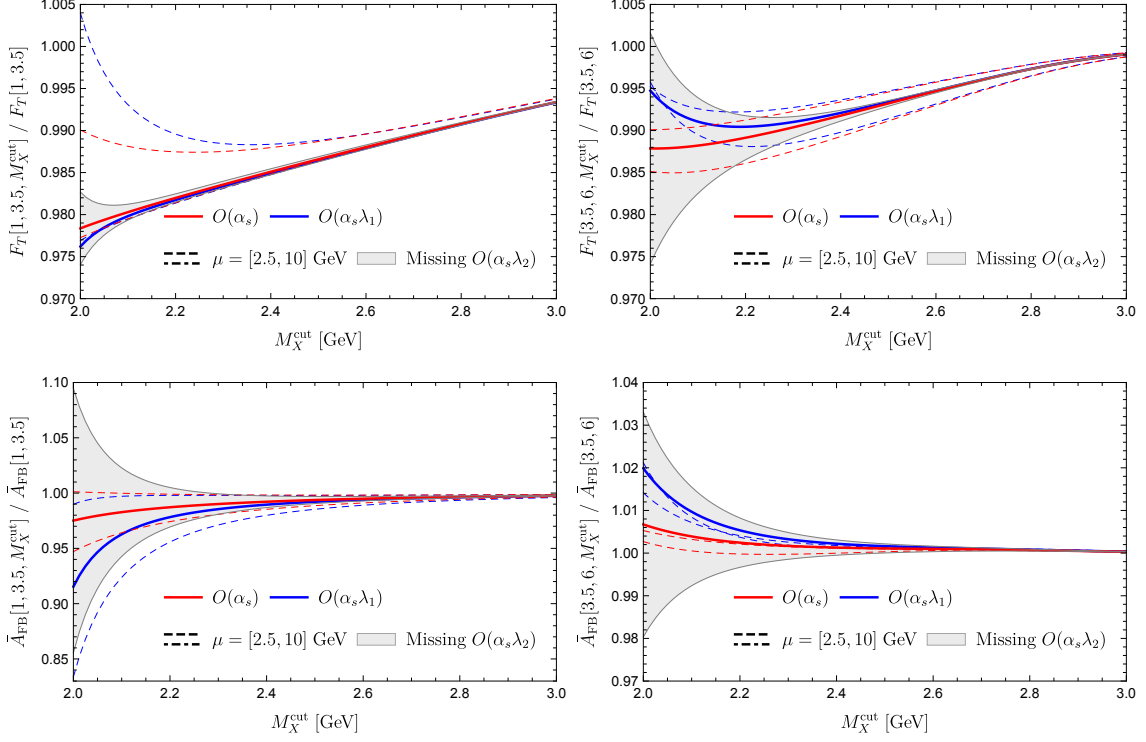


Figure 5: Impact of a cut on the hadronic invariant mass on the low- q^2 normalized angular observables. See the caption in figure 2 for further details.

$$\bar{A}_{\text{FB}}[q_1^2, q_2^2] = \frac{\int_{s_1}^{s_2} ds \int_0^{(1-\sqrt{s})^2} du \frac{3}{4} \frac{d^2 \mathcal{H}_A}{ds du}}{\int_{s_1}^{s_2} ds \int_0^{(1-\sqrt{s})^2} du \frac{d^2 \mathcal{B}}{ds du}}, \quad (3.12)$$

and

$$F_T[q_1^2, q_2^2, M_X^{\text{cut}}] = \frac{\int_{s_1}^{s_2} ds \int_0^{(1-\sqrt{s})^2} du \theta(M_X^{\text{cut}} - M_X) \frac{d^2 \mathcal{H}_T}{ds du}}{\int_{s_1}^{s_2} ds \int_0^{(1-\sqrt{s})^2} du \theta(M_X^{\text{cut}} - M_X) \frac{d^2 \mathcal{B}}{ds du}}, \quad (3.13)$$

$$F_T[q_1^2, q_2^2] = \frac{\int_{s_1}^{s_2} ds \int_0^{(1-\sqrt{s})^2} du \frac{d^2 \mathcal{H}_T}{ds du}}{\int_{s_1}^{s_2} ds \int_0^{(1-\sqrt{s})^2} du \frac{d^2 \mathcal{B}}{ds du}}. \quad (3.14)$$

The first important point to notice is that the $O(\alpha_s)$ corrections are $O(1\%)$, an order of magnitude smaller than for the rates presented in figures 2, 3 and 4. The reason for this behavior can be traced to the leading power results in eq. (3.2), where it is apparent that the $1/u$ singularities are universal to all angular observables. Upon integration, the

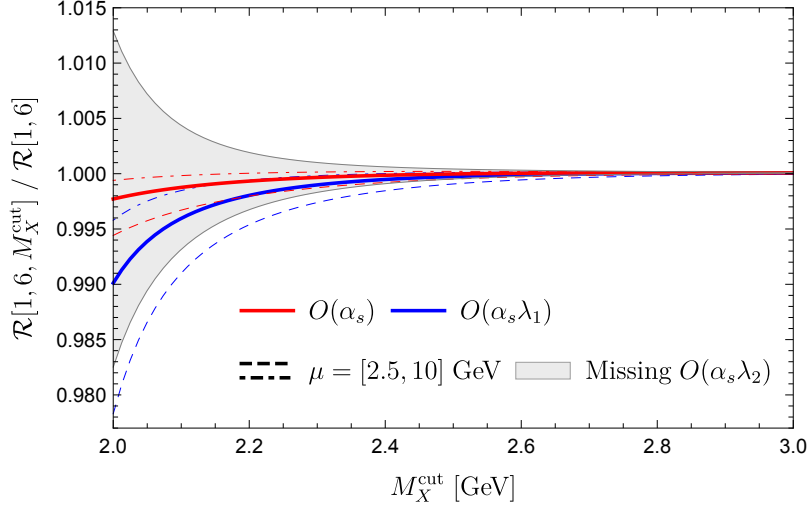


Figure 6: Impact of a cut on the hadronic invariant mass on the low- q^2 observable \mathcal{R} . See the caption in figure 2 for further details.

resulting logarithms of M_X^{cut} appearing in the numerator and denominator of F_T and \bar{A}_{FB} therefore cancel. Power corrections at $O(\alpha_s \lambda_1/m_b^2)$ are also quite small because $1/u^3$ and $1/u^2$ singular terms in eq. (3.5) are universal. This universality is lost for $O(\alpha_s \lambda_2/m_b^2)$ corrections. The latter, therefore, can potentially have a larger impact on these normalized ratios. In conclusion, the gray bands in figure 5 might underestimate the potential size of missing $O(\alpha_s \lambda_2/m_b^2)$ effects, especially at small values of M_X^{cut} . This issue will be clarified when the $O(\alpha_s \lambda_2/m_b^2)$ corrections are available.

The panel for the observable $F_T[1, 3.5]$ appears to be exceptional, in that even for $M_X^{\text{cut}} = 2.0$ GeV, the $O(\alpha_s \lambda_1/m_b^2)$ correction is smaller than the $O(\alpha_s)$ correction, but this seems to originate from a cancellation that holds only at $\mu_b = 5$ GeV (as it is apparent from inspection of the $\mu_b = 2.5$ GeV dashed curves). In general, the shifts observed as the scale μ_b is varied in the $[2.5, 10]$ GeV interval are also quite asymmetric for all observables because of various correlations between the numerator and denominators of F_T and \bar{A}_{FB} .

Finally, we consider the ratio formed by normalizing the $\bar{B} \rightarrow X_s \ell^+ \ell^-$ branching fraction to the branching fraction of $\bar{B} \rightarrow X_u \ell^- \nu$ with the same q^2 and M_X cuts. Such a ratio was introduced in [47] to analyze the high- q^2 region. Here we study its dependence on the hadronic mass cut in the low- q^2 region, as proposed in [34],

$$\mathcal{R}[q_1^2, q_2^2, M_X^{\text{cut}}] = \frac{\int_{s_1}^{s_2} ds \int_0^{(1-\sqrt{s})^2} du \theta(M_X^{\text{cut}} - M_X) \frac{d^2 \mathcal{B}(\bar{B} \rightarrow X_s \ell^+ \ell^-)}{ds du}}{\int_{s_1}^{s_2} ds \int_0^{(1-\sqrt{s})^2} du \theta(M_X^{\text{cut}} - M_X) \frac{d^2 \mathcal{B}(\bar{B} \rightarrow X_u \ell^- \nu)}{ds du}}, \quad (3.15)$$

$$\mathcal{R}[q_1^2, q_2^2] = \frac{\int_{s_1}^{s_2} ds \int_0^{(1-\sqrt{s})^2} du \frac{d^2 \mathcal{B}(\bar{B} \rightarrow X_s \ell^+ \ell^-)}{ds du}}{\int_{s_1}^{s_2} ds \int_0^{(1-\sqrt{s})^2} du \frac{d^2 \mathcal{B}(\bar{B} \rightarrow X_u \ell^- \nu)}{ds du}}. \quad (3.16)$$

In the $C_7 \rightarrow 0$ limit, $\bar{B} \rightarrow X_u \ell^- \nu$ and $\bar{B} \rightarrow X_s \ell^+ \ell^-$ have the same hadronic mass spectra in QCD, to all orders in α_s and to all orders in $1/m_b$. While the $O(1\%)$ sensitivity of this observable to the hadronic mass cut shown in figure 6 is similar to that of F_T and \bar{A}_{FB} , it is important to observe that the cancellation of the M_X^{cut} dependence between numerators and denominators is different in the two cases. For the ratio \mathcal{R} , terms proportional to $|C_9^{\text{eff}}|^2 + |C_{10}|^2$ are completely independent of M_X^{cut} and the small cut dependence is controlled by terms involving C_7 , which are subleading in the $\bar{B} \rightarrow X_s \ell^+ \ell^-$ rate by a factor $|4C_7 C_9| / (C_9^2 + C_{10}^2) \sim 0.15$.

4 Conclusions

Measurements of the branching fractions and angular observables of inclusive $\bar{B} \rightarrow X_s \mu^+ \mu^-$ and $\bar{B} \rightarrow X_s e^+ e^-$, with precision competitive for the first time with SM predictions, are finally on the horizon [25]. To make the most of rare decay modes at Belle II, it is important at this time to reflect on the results from the first generation B factories and pinpoint what observables are both straightforward to measure with high statistics and low backgrounds, and what observables are sensitive to physics beyond the SM with minimal interference from nonperturbative QCD.

In this context, the most important conceptual advancement that can be made in the phenomenology of $\bar{B} \rightarrow X_s \ell^+ \ell^-$ at low- q^2 is to improve or replace the procedure of extrapolating out of the signal region $M_X \lesssim 2.0 \text{ GeV}$, historically done on the experimental side, in order to compare with SM predictions without a hadronic mass cut. The observables \bar{A}_{FB} , F_T and \mathcal{R} are significantly less sensitive to the hadronic mass cut than the standard angular observables, since they are formed from ratios of observables for which the hadronic mass spectrum is universal to an excellent approximation. The main conclusion of our study is that for $M_X^{\text{cut}} \gtrsim 2.5 \text{ GeV}$, this cut dependence may be calculated with an OPE. Since cuts in the OPE region are difficult to realize experimentally, a complementary calculation for cuts in the shape function region within SCET is planned, supplemented with an interpolation between shape function and OPE regions.

In conclusion, the angular observables $\mathcal{H}_T, \mathcal{H}_A, \mathcal{H}_L$ of $\bar{B} \rightarrow X_s \ell^+ \ell^-$ should be measured together with the branching fraction of $\bar{B} \rightarrow X_u \ell^- \nu$, with the same cuts on q^2 and M_X , without extrapolation in M_X^{cut} . The data on $\bar{B} \rightarrow X_u \ell^- \nu$ is helpful in reducing the effect of the hadronic mass cut on the extraction of the Wilson coefficients of $\bar{B} \rightarrow X_s \ell^+ \ell^-$. A breakdown into bins of M_X would be helpful, especially for the bins at $M_X \sim 2.0 \text{ GeV}$ which are affected by large backgrounds. It is critical that all results are presented with correlations, since the ideal observables on the theory side are ratios of linear combinations of these branching fractions.

Acknowledgements

The research of T. Huber was supported by the Deutsche Forschungsgemeinschaft (DFG, German Research Foundation) under grant 396021762 – TRR 257 “Particle Physics Phenomenology after the Higgs Discovery.” T. Hurth is supported by the Cluster of Excellence “Precision Physics, Fundamental Interactions, and Structure of Matter” (PRISMA⁺ EXC 2118/1) funded by the German Research Foundation (DFG) within the German Excellence Strategy (Project ID 39083149). T. Hurth also thanks the CERN theory group for its hospitality during his regular visits to CERN where part of the work was done.

A Analytical results

A.1 Integrals

The NLO matrix elements were reduced using IBP techniques with FeynCalc [48] and FIRE [49]. The following master integral appears in the computation of the NLO matrix element:

$$M_{a_1, a_2, a_3} = -\frac{1}{\pi} \text{Im} \left[\frac{1}{u} \int \frac{\tilde{d}k}{[k^2]^{a_1} [(k - \hat{p})^2]^{a_2} [(k + \hat{q})^2 - 1]^{a_3}} \right], \quad (\text{A.1})$$

where $\tilde{d}k = d^{4-2\epsilon} k e^{\epsilon\gamma_E} / (i\pi^{2-\epsilon})$, $\hat{p} = (m_b v - q)/m_b$, $\hat{q} = q/m_b$, and k is already rescaled to be dimensionless. After partial fractions and IBP reduction, the integrals needed are M_{001} , M_{110} , M_{101} and M_{111} . The results are

$$M_{001} = \left(\frac{1}{\epsilon} + 1 \right) \delta(u), \quad (\text{A.2})$$

$$M_{101} = \left(\frac{1}{\epsilon} + \frac{w \ln w}{1-w} + 2 \right) \delta(u), \quad (\text{A.3})$$

$$M_{110} = \left(\frac{1}{\epsilon} + 2 \right) \delta(u) - \left[\frac{1}{u} \right]_+, \quad (\text{A.4})$$

$$M_{111} = -\frac{1}{w} \left(\text{Li}_2(1-w) + 2 \ln^2 w + \frac{\pi^2}{3} \right) \delta(u) + \left[\frac{\mathcal{I}}{u} \right]_+, \quad (\text{A.5})$$

where \mathcal{I} is given in eq. (2.6). In terms of standard distributions,

$$\left[\frac{\mathcal{I}}{u} \right]_+ = -\frac{1}{w} \left[\frac{\ln u}{u} \right]_+ + \frac{2 \ln w}{w} \left[\frac{1}{u} \right]_+ + \frac{1}{u} \left(\mathcal{I} + \frac{1}{w} \ln \frac{u}{w^2} \right) \theta(u). \quad (\text{A.6})$$

All $1/\epsilon$ divergences are UV in origin. M_{001} and M_{101} are proportional to $\delta(u)$, since the loop integrals are real and elementary to evaluate. M_{110} depends only on a single scale u and is also elementary. For $u > 0$, eq. (A.5) can be confirmed by introducing Feynman parameters, using $-(1/\pi) \text{Im}[1/\Delta] = \delta(\Delta)$, and integrating over Feynman parameters,

$$M_{111}(u > 0) = \frac{1}{u} \int_0^1 dx_1 \int_0^1 dx_2 \delta \left[x_1 \bar{x}_2 u - \bar{x}_1 x_2 (\bar{x}_1 + x_1 w) \right] = \frac{\mathcal{I}}{u}. \quad (\text{A.7})$$

Here and in the following, for any variable z we introduce $\bar{z} = 1 - z$. The coefficients of the plus distributions are also inferred from this exercise by extracting the $u \rightarrow 0$ behavior of the $u > 0$ result, obtaining an ansatz

$$M_{111} = M_{111}^\delta \delta(u) + \left[\frac{\mathcal{I}}{u} \right]_+ \quad (\text{A.8})$$

in terms of an undetermined coefficient. To extract this coefficient, we combine the $1/u$ prefactor into the integral using a third Feynman parameter, integrate on the interval $u \in [0, U]$, remove the regulator ϵ (U now serves as an IR regulator) and expand in $U \rightarrow 0$:

$$\begin{aligned} \int_0^U du M_{111} &= - \int_0^1 dx_1 \int_0^1 dx_2 \int_0^1 dx_3 \frac{\delta \left[(x_1 \bar{x}_2 x_3 + \bar{x}_3) U - \bar{x}_1 x_2 x_3 (\bar{x}_1 + x_1 w) \right]}{x_1 \bar{x}_2 x_3 + \bar{x}_3} \\ &= - \int_0^1 dx_1 \frac{1}{\bar{x}_1 (1 - \bar{w} x_1)} \ln \left(1 + \frac{\bar{x}_1 (1 - \bar{w} x_1)}{U x_1} \right) \\ &= - \int_{c_1 - i\infty}^{c_1 + i\infty} \frac{dz_1}{2\pi i} \int_{c_2 - i\infty}^{c_2 + i\infty} \frac{dz_2}{2\pi i} \frac{\Gamma(z_1 + 1) \Gamma(-z_2) \Gamma(1 + 2z_1 - z_2) \Gamma^2(z_2 - z_1)}{\Gamma(z_1 + 2)} U^{-z_1 - 1} w^{z_2}. \end{aligned} \quad (\text{A.9})$$

The Mellin-Barnes representation in the third line is well-suited for extracting the asymptotic behavior for $U \rightarrow 0$ to any desired order [50, 51]. The values $c_1 = -3/8$ and $c_2 = -1/4$ denote the constant real parts of the integration contours in the complex plane. One obtains

$$\int_0^U du M_{111} = -\frac{1}{w} \left(\text{Li}_2(1 - w) + 2 \ln^2 w + \frac{\pi^2}{3} \right) - \frac{\ln^2 U}{2w} + \frac{2 \ln w}{w} \ln U + O(U). \quad (\text{A.10})$$

The constant term in this expression extracts the coefficient of the delta function in eq. (A.5) respectively eq. (A.8).

A.2 Form factors

In this appendix, the eight form factors h_f^{ij} are given as an expansion in α_s and $1/m_b$, up to $O(\alpha_s \lambda_1 / m_b^2)$. The $O(\alpha_s)$ and $O(\alpha_s \lambda_1 / m_b^2)$ corrections are proportional to $C_F = 4/3$. The following terms always appear together in the combination

$$L_w = \text{Li}_2(1 - w) + 2 \ln^2 w + \frac{\pi^2}{3} + \frac{1}{4} \{0, 1, 2\} \ln \frac{\mu_b^2}{m_b^2}. \quad (\text{A.11})$$

The bracket notation indicates the $ij = \{99, 79, 77\}$ interference (in the case of h_A^{ij} , the last entry is deleted and $ij = \{90, 70\}$).

A.2.1 $O(\lambda_1 / m_b^2)$

$$\left\{ h_{T,\delta}^{99(\lambda_1,0)}, h_{T,\delta}^{79(\lambda_1,0)}, h_{T,\delta}^{77(\lambda_1,0)} \right\} = \frac{1}{2} - \frac{4}{3w} \{1, 0, w - 1\}, \quad (\text{A.12})$$

$$\left\{ h_{A,\delta}^{90(\lambda_1,0)}, h_{A,\delta}^{70(\lambda_1,0)} \right\} = \frac{1}{2} + \frac{4}{3w^2} \{1 - w, 1 - w\}, \quad (\text{A.13})$$

$$\left\{ h_{L,\delta}^{99(\lambda_1,0)}, h_{L,\delta}^{79(\lambda_1,0)}, h_{L,\delta}^{77(\lambda_1,0)} \right\} = \frac{1}{2} - \frac{8}{3w} \{w - 1, 0, 1\}. \quad (\text{A.14})$$

A.2.2 $O(\alpha_s)$

$$\left\{ h_{T,\delta}^{99(1)}, h_{T,\delta}^{79(1)}, h_{T,\delta}^{77(1)} \right\} = -C_F \left(4L_w - 8 \ln w + 5 + \left\{ 2, 1, 0 \right\} \frac{w \ln w}{1-w} \right), \quad (\text{A.15})$$

$$\left\{ h_{A,\delta}^{90(1)}, h_{A,\delta}^{70(1)} \right\} = -C_F \left(4L_w - 8 \ln w + 5 + \left\{ 2, 1 \right\} \frac{w \ln w}{1-w} \right), \quad (\text{A.16})$$

$$\left\{ h_{L,\delta}^{99(1)}, h_{L,\delta}^{79(1)}, h_{L,\delta}^{77(1)} \right\} = -C_F \left(4L_w - 8 \ln w + 5 + \left\{ 0, 2, 4 \right\} \frac{w \ln w}{1-w} \right), \quad (\text{A.17})$$

$$\begin{aligned} \left\{ h_{T,\theta}^{99(1)}, h_{T,\theta}^{79(1)}, h_{T,\theta}^{77(1)} \right\} &= \frac{4C_F}{u} \left[\ln \frac{u}{w^2} + \sqrt{\lambda} \mathcal{I} + \frac{7}{4} \left(1 - \frac{\sqrt{\lambda}}{w} \right) \right] \\ &+ \frac{2C_F \mathcal{I}}{w^2 \sqrt{\lambda}} \left\{ \begin{array}{l} 2w^3 - w(14 - 5w)u - 4(2 - w)u^2 + u^3, \\ 2w^3 - w(9 - 4w)u + (1 + 2w)u^2, \\ 2w^3 - w(4 + w)u + 2(3 - w)u^2 - u^3 \end{array} \right\} \\ &+ \frac{C_F}{w^2 \sqrt{\lambda}} \left\{ \begin{array}{l} 3w^2 + 4(3 + w)u + u^2, \\ 2(2 - w)u - 2u^2, \\ -w^2(3 - 2w) - 4(1 - w - w^2)u - (9 - 4w)u^2 + 2u^3 \end{array} \right\}, \end{aligned} \quad (\text{A.18})$$

$$\begin{aligned} \left\{ h_{A,\theta}^{90(1)}, h_{A,\theta}^{70(1)} \right\} &= \frac{4C_F}{u} \left[\ln \frac{u}{w^2} + w \mathcal{I} \right] - \frac{2C_F \mathcal{I}}{w^2} \left\{ \begin{array}{l} 4w(1 - w) + 3(2 - w)u - u^2, \\ 4w(1 - w) + (5 - 2w)u \end{array} \right\} \\ &+ \frac{C_F}{w^2} \left\{ \begin{array}{l} 12 - 4w - u, \\ 12 - 5w + 2u \end{array} \right\}, \end{aligned} \quad (\text{A.19})$$

$$\begin{aligned} \left\{ h_{L,\theta}^{99(1)}, h_{L,\theta}^{79(1)}, h_{L,\theta}^{77(1)} \right\} &= \frac{4C_F}{u} \left[\ln \frac{u}{w^2} + \sqrt{\lambda} \mathcal{I} + \frac{7}{4} \left(1 - \frac{\sqrt{\lambda}}{w} \right) \right] \\ &+ \frac{2C_F \mathcal{I}}{w^2 \sqrt{\lambda}} \left\{ \begin{array}{l} 2w^3 + w(4 - 7w)u + 4(1 - w)u^2 + u^3, \\ 2w^3 - 3w(2 - w)u + 2u^2 - u^3, \\ 2w^3 - w(16 - 5w)u - 4(2 - w)u^2 + u^3 \end{array} \right\} \\ &+ \frac{C_F}{w^2 \sqrt{\lambda}} \left\{ \begin{array}{l} -w^2(7 - 4w) - 2(10 - 11w - 2w^2)u - 3u^2, \\ -w^2 - 2(2 - w)u + 3u^2, \\ 5w^2 + 6(2 + w)u + u^2 \end{array} \right\}. \end{aligned} \quad (\text{A.20})$$

A.2.3 $O(\alpha_s \lambda_1 / m_b^2)$

$$\left\{ h_{T, [\ln/1]}^{99(\lambda_1, 1)}, h_{T, [\ln/1]}^{79(\lambda_1, 1)}, h_{T, [\ln/1]}^{77(\lambda_1, 1)} \right\} = -2C_F \left(1 - \frac{8}{3w} \left\{ 1, 0, w - 1 \right\} \right), \quad (\text{A.21})$$

$$\left\{ h_{A, [\ln/1]}^{90(\lambda_1, 1)}, h_{A, [\ln/1]}^{70(\lambda_1, 1)} \right\} = -2C_F \left(1 + \frac{8}{3w^2} \left\{ 1 - w, 1 - w \right\} \right), \quad (\text{A.22})$$

$$\left\{ h_{L, [\ln/1]}^{99(\lambda_1, 1)}, h_{L, [\ln/1]}^{79(\lambda_1, 1)}, h_{L, [\ln/1]}^{77(\lambda_1, 1)} \right\} = -2C_F \left(1 - \frac{16}{3w} \left\{ w - 1, 0, 1 \right\} \right), \quad (\text{A.23})$$

$$\left\{ h_{T,[/1]}^{99(\lambda_1,1)}, h_{T,[/1]}^{79(\lambda_1,1)}, h_{T,[/1]}^{77(\lambda_1,1)} \right\} = \frac{C_F}{6w} \begin{pmatrix} 52 - 31w, \\ 6 - 33w, \\ -40 + 13w \end{pmatrix} + \frac{4C_F}{3} \begin{pmatrix} -8 + 3w, \\ 3w, \\ 8 - 5w \end{pmatrix} \frac{\ln w}{w}, \quad (\text{A.24})$$

$$\left\{ h_{A,[/1]}^{90(\lambda_1,1)}, h_{A,[/1]}^{70(\lambda_1,1)} \right\} = \frac{C_F}{6w^2} \begin{pmatrix} -48 + 52w - 31w^2, \\ -48 + 54w - 33w^2 \end{pmatrix} + \frac{4C_F}{3} \begin{pmatrix} 8 - 8w + 3w^2, \\ 8 - 8w + 3w^2 \end{pmatrix} \frac{\ln w}{w^2}, \quad (\text{A.25})$$

$$\left\{ h_{L,[/1]}^{99(\lambda_1,1)}, h_{L,[/1]}^{79(\lambda_1,1)}, h_{L,[/1]}^{77(\lambda_1,1)} \right\} = \frac{C_F}{6w} \begin{pmatrix} -80 + 57w, \\ 12 - 35w, \\ 104 - 31w \end{pmatrix} + \frac{4C_F}{3} \begin{pmatrix} 16 - 13w, \\ 3w, \\ -16 + 3w \end{pmatrix} \frac{\ln w}{w}, \quad (\text{A.26})$$

$$\left\{ h_{T,\delta\prime\prime}^{99(\lambda_1,1)}, h_{T,\delta\prime\prime}^{79(\lambda_1,1)}, h_{T,\delta\prime\prime}^{77(\lambda_1,1)} \right\} = \frac{2C_F w^2}{3} \left(L_w + \ln w - \frac{7}{8} + \frac{1}{4} \{2, 1, 0\} \frac{w \ln w}{1-w} \right), \quad (\text{A.27})$$

$$\left\{ h_{A,\delta\prime\prime}^{90(\lambda_1,1)}, h_{A,\delta\prime\prime}^{70(\lambda_1,1)} \right\} = \frac{2C_F w^2}{3} \left(L_w + \ln w - \frac{7}{8} + \frac{1}{4} \{2, 1\} \frac{w \ln w}{1-w} \right), \quad (\text{A.28})$$

$$\left\{ h_{L,\delta\prime\prime}^{99(\lambda_1,1)}, h_{L,\delta\prime\prime}^{79(\lambda_1,1)}, h_{L,\delta\prime\prime}^{77(\lambda_1,1)} \right\} = \frac{2C_F w^2}{3} \left(L_w + \ln w - \frac{7}{8} + \frac{1}{2} \{0, 1, 2\} \frac{w \ln w}{1-w} \right), \quad (\text{A.29})$$

$$\begin{aligned} \left\{ h_{T,\delta\prime}^{99(\lambda_1,1)}, h_{T,\delta\prime}^{79(\lambda_1,1)}, h_{T,\delta\prime}^{77(\lambda_1,1)} \right\} &= 2C_F(2-w)L_w - \frac{C_F}{6} \begin{pmatrix} 30 - 4w - 10w^2, \\ 30 - 7w - 10w^2, \\ 30 - 10w - 8w^2 \end{pmatrix} \\ &+ \frac{C_F}{6} \begin{pmatrix} 32 - 44w + 2w^2 + 16w^3, \\ 32 - 50w + 5w^2 + 16w^3, \\ 32 - 56w + 8w^2 + 16w^3 \end{pmatrix} \frac{\ln w}{1-w}, \end{aligned} \quad (\text{A.30})$$

$$\begin{aligned} \left\{ h_{A,\delta\prime}^{90(\lambda_1,1)}, h_{A,\delta\prime}^{70(\lambda_1,1)} \right\} &= 2C_F(2-w)L_w - \frac{C_F}{6} \begin{pmatrix} 28 - 4w - 10w^2, \\ 28 - 5w - 10w^2 \end{pmatrix} \\ &+ \frac{C_F}{6} \begin{pmatrix} 32 - 44w + 2w^2 + 16w^3, \\ 32 - 50w + 5w^2 + 16w^3 \end{pmatrix} \frac{\ln w}{1-w}, \end{aligned} \quad (\text{A.31})$$

$$\begin{aligned} \left\{ h_{L,\delta\prime}^{99(\lambda_1,1)}, h_{L,\delta\prime}^{79(\lambda_1,1)}, h_{L,\delta\prime}^{77(\lambda_1,1)} \right\} &= 2C_F(2-w)L_w - \frac{C_F}{6} \begin{pmatrix} 30 - 14w - 6w^2, \\ 30 - 8w - 10w^2, \\ 30 - 2w - 10w^2 \end{pmatrix} \\ &+ \frac{C_F}{6} \begin{pmatrix} 32 - 56w + 8w^2 + 16w^3, \\ 32 - 44w + 2w^2 + 16w^3, \\ 32 - 32w - 4w^2 + 16w^3 \end{pmatrix} \frac{\ln w}{1-w}, \end{aligned} \quad (\text{A.32})$$

$$\left\{ h_{T,\delta}^{99(\lambda_1,1)}, h_{T,\delta}^{79(\lambda_1,1)}, h_{T,\delta}^{77(\lambda_1,1)} \right\} = \frac{2C_F}{3w} L_w \{8 - 3w, -3w, -8 + 5w\}$$

$$\begin{aligned}
& -\frac{C_F}{6w^2} \left\{ \begin{array}{l} 14 + 2w - 10w^2 + 9w^3 + 3w^4, \\ 14 + 12w - 8w^2 + 9w^3 + 3w^4, \\ 14 + 22w - 18w^2 + 9w^3 + 3w^4 \end{array} \right\} \\
& -\frac{C_F}{6w} \left\{ \begin{array}{l} 72 - 68w - 22w^2 + 16w^3 + 8w^4, \\ 4 - 4w - 21w^2 + 16w^3 + 8w^4, \\ -64 + 140w - 100w^2 + 16w^3 + 8w^4 \end{array} \right\} \frac{\ln w}{1-w}, \tag{A.33}
\end{aligned}$$

$$\begin{aligned}
\left\{ h_{A,\delta}^{90(\lambda_1,1)}, h_{A,\delta}^{70(\lambda_1,1)} \right\} &= -\frac{2C_F}{3w^2} L_w(8 - 8w + 3w^2) - \frac{C_F}{6w^2} \left\{ \begin{array}{l} 28 - 12w^2 + 9w^3 + 3w^4, \\ 28 - 4w - 6w^2 + 9w^3 + 3w^4 \end{array} \right\} \\
&+ \frac{C_F}{6w^2} \left\{ \begin{array}{l} 48 - 120w + 68w^2 + 22w^3 - 16w^4 - 8w^5, \\ 48 - 116w + 68w^2 + 21w^3 - 16w^4 - 8w^5 \end{array} \right\} \frac{\ln w}{1-w}, \tag{A.34}
\end{aligned}$$

$$\begin{aligned}
\left\{ h_{L,\delta}^{99(\lambda_1,1)}, h_{L,\delta}^{79(\lambda_1,1)}, h_{L,\delta}^{77(\lambda_1,1)} \right\} &= \frac{2C_F}{3w} L_w \left\{ -16 + 13w, -3w, 16 - 3w \right\} \\
&- \frac{C_F}{6w^2} \left\{ \begin{array}{l} 14 + 14w - 12w^2 + 5w^3 + 3w^4, \\ 14 - 6w + 9w^3 + 3w^4, \\ 14 - 26w - 12w^2 + 9w^3 + 3w^4 \end{array} \right\} \\
&- \frac{C_F}{6w} \left\{ \begin{array}{l} -96 + 212w - 140w^2 + 16w^3 + 8w^4, \\ 40 - 44w - 14w^2 + 16w^3 + 8w^4, \\ 176 - 172w - 16w^2 + 16w^3 + 8w^4 \end{array} \right\} \frac{\ln w}{1-w}, \tag{A.35}
\end{aligned}$$

$$\begin{aligned}
\left\{ h_{T,\theta}^{99(\lambda_1,1)}, h_{T,\theta}^{79(\lambda_1,1)}, h_{T,\theta}^{77(\lambda_1,1)} \right\} &= -\frac{2C_F}{3wu^3} \left\{ \begin{array}{l} 2w^3 - 3w(2-w)u + (8-3w)u^2, \\ 2w^3 - 3w(2-w)u - 3wu^2, \\ 2w^3 - 3w(2-w)u - (8-5w)u^2 \end{array} \right\} \ln \frac{u}{w^2} \\
&- \frac{C_F \mathcal{I}}{3w^2 u^3 \sqrt{\lambda}} \left\{ \begin{array}{l} 4w^6 - 14w^4(2-w)u + 2w^2(24-16w+5w^2)u^2 \\ -w(36-36w+13w^2)u^3 - (8-58w+23w^2)u^4 \\ +13(2-w)u^5 - 3u^6, \\ 4w^6 - 14w^4(2-w)u + 2w^2(24-24w+5w^2)u^2 \\ -w(6-17w+14w^2)u^3 - (4-41w+22w^2)u^4 \\ -4(1+2w)u^5, \\ 4w^6 - 14w^4(2-w)u + 2w^2(24-32w+13w^2)u^2 \\ +w(24-34w+9w^2)u^3 + (16-8w+3w^2)u^4 \\ -(18-5w)u^5 + 3u^6 \end{array} \right\} \\
&- \frac{C_F}{6wu^3} \left\{ \begin{array}{l} 2w^3 - w(2+3w)u + (52-31w)u^2, \\ 2w^3 - w(2+3w)u + (6-33w)u^2, \\ 2w^3 - w(2+3w)u - (40-13w)u^2 \end{array} \right\}
\end{aligned}$$

$$+ \frac{C_F}{6w^2u^3\sqrt{\lambda}} \left\{ \begin{array}{l} 2w^5 - w^3(22 - 15w)u + 2w(28 - 14w - w^2)u^2 \\ -(64 - 110w + 34w^2)u^3 + 4(17 - 5w)u^4 - u^5, \\ 2w^5 - w^3(22 - 15w)u + 2w(28 - 37w - 2w^2)u^2 \\ -(16 - 116w + 43w^2)u^3 + 8(1 - 4w)u^4 - 6u^5, \\ 2w^5 - w^3(22 - 15w)u + 2w(28 - 60w + 21w^2)u^2 \\ + 2(16 + 37w - 22w^2 + w^3)u^3 - 4(17 - 7w + w^2)u^4 \\ + (13 - 6w)u^5 \end{array} \right\}, \quad (\text{A.36})$$

$$\left\{ h_{A,\theta}^{90(\lambda_1,1)}, h_{A,\theta}^{70(\lambda_1,1)} \right\} = -\frac{2C_F}{3w^2u^3} \left\{ \begin{array}{l} 2w^4 - 3w^2(2 - w)u - (8 - 8w + 3w^2)u^2, \\ 2w^4 - 3w^2(2 - w)u - (8 - 8w + 3w^2)u^2 \end{array} \right\} \ln \frac{u}{w^2}$$

$$- \frac{C_F \mathcal{I}}{3w^2u^3} \left\{ \begin{array}{l} 4w^5 - 10w^3(2 - w)u - (12 - 24w + 13w^2)u^3 + 10(2 - w)u^4 - 3u^5, \\ 4w^5 - 10w^3(2 - w)u - (10 - 21w + 14w^2)u^3 + 4(5 - 2w)u^4 \end{array} \right\}$$

$$- \frac{C_F}{6w^2u^2} \left\{ \begin{array}{l} 16w^2(1 - w) - 8(1 - w)(3 - 2w)u - (54 - 17w)u^2 + 7u^3, \\ 16w^2(1 - w) - 8(1 - w)(3 - 2w)u - (52 - 22w)u^2 - 6u^3 \end{array} \right\}, \quad (\text{A.37})$$

$$\left\{ h_{L,\theta}^{99(\lambda_1,1)}, h_{L,\theta}^{79(\lambda_1,1)}, h_{L,\theta}^{77(\lambda_1,1)} \right\} = -\frac{2C_F}{3wu^3} \left\{ \begin{array}{l} 2w^3 - 3w(2 - w)u - (16 - 13w)u^2, \\ 2w^3 - 3w(2 - w)u - 3wu^2, \\ 2w^3 - 3w(2 - w)u + (16 - 3w)u^2 \end{array} \right\} \ln \frac{u}{w^2}$$

$$- \frac{C_F \mathcal{I}}{3w^2u^3\sqrt{\lambda}} \left\{ \begin{array}{l} 4w^6 - 14w^4(2 - w)u + 2w^2(24 - 40w + 21w^2)u^2 \\ + 3w(24 - 38w + 13w^2)u^3 + (40 - 76w + 45w^2)u^4 \\ - (22 - 19w)u^5 - 3u^6, \\ 4w^6 - 14w^4(2 - w)u + 2w^2(24 - 24w + 5w^2)u^2 \\ + w(12 + 4w - 15w^2)u^3 + w(22 - 21w)u^4 \\ - (2 + 3w)u^5 + 3u^6, \\ 4w^6 - 14w^4(2 - w)u + 2w^2(24 - 8w + 5w^2)u^2 \\ - w(48 - 58w + 13w^2)u^3 - (40 - 72w + 23w^2)u^4 \\ + 13(2 - w)u^5 - 3u^6 \end{array} \right\}$$

$$- \frac{C_F}{6wu^3} \left\{ \begin{array}{l} 2w^3 - w(2 + 3w)u - (80 - 57w)u^2, \\ 2w^3 - w(2 + 3w)u + (12 - 35w)u^2, \\ 2w^3 - w(2 + 3w)u + (104 - 31w)u^2 \end{array} \right\}$$

$$+ \frac{C_F}{6w^2u^3\sqrt{\lambda}} \left\{ \begin{array}{l} 2w^5 - w^3(22 - 15w)u + 2w(28 - 80w + 43w^2)u^2 \\ + 2(64 - 39w - 15w^2 + 8w^3)u^3 \\ - (76 - 60w - 16w^2)u^4 - 13u^5, \\ 2w^5 - w^3(22 - 15w)u + 2w(28 - 34w - 3w^2)u^2 \\ + (32 + 70w - 52w^2)u^3 - 20(1 + w)u^4 + 13u^5, \\ 2w^5 - w^3(22 - 15w)u + 2w(28 + 12w - w^2)u^2 \\ - (64 - 90w + 26w^2)u^3 + 12(3 - w)u^4 - u^5 \end{array} \right\}. \quad (\text{A.38})$$

A.3 Hadronic tensors

The leading order, $O(\alpha_s)$ and $O(\alpha_s \lambda_1/m_b^2)$ contributions to the functions W_a^{ij} appearing in eq. (2.19) can be expressed as:

$$W_a^{ij} = W_a^{ij(0)} - \frac{\lambda_1}{2m_b^2} W_a^{ij(\lambda_1,0)} + \frac{\alpha_s C_F}{4\pi} \left[W_a^{ij(1)} - \frac{\lambda_1}{2m_b^2} W_a^{ij(\lambda_1,1)} \right]. \quad (\text{A.39})$$

We present the explicit results for the leading order and $O(\alpha_s)$ contributions in terms of the variables $w = 1 - \hat{q}^2$ and $u = (v - \hat{q})^2$, where $\hat{q} = q/m_b$ and $v = p_B/M_B$. The tree level results are

$$W_a^{ij(0)} = W_{a,\delta}^{ij(0)} \delta(u), \quad (\text{A.40})$$

where

$$\left\{ W_{1,\delta}^{99(0)}, W_{2,\delta}^{99(0)}, W_{3,\delta}^{99(0)} \right\} = \left\{ \frac{w}{4}, 1, \frac{1}{2} \right\}, \quad (\text{A.41})$$

$$\left\{ W_{1,\delta}^{79(0)}, W_{2,\delta}^{79(0)}, W_{3,\delta}^{79(0)} \right\} = \frac{1}{1-w} \left\{ \frac{w}{2}, 0, 1 \right\}, \quad (\text{A.42})$$

$$\left\{ W_{1,\delta}^{77(0)}, W_{2,\delta}^{77(0)}, W_{3,\delta}^{77(0)} \right\} = \frac{1}{(1-w)^2} \{w, -4(1-w), 2\}. \quad (\text{A.43})$$

The $O(\alpha_s)$ results are

$$\begin{aligned} W_a^{ij(1)} = & W_{a,\delta}^{ij(0)} \left(-4 \left[\frac{\ln u}{u} \right]_+ + (8 \ln w - 7) \left[\frac{1}{u} \right]_+ + \mathcal{S} \delta(u) + \frac{4}{u} \ln \frac{u}{w^2} \theta(u) \right) \\ & + W_{a,\delta}^{ij(1)} \delta(u) + W_{a,\theta}^{ij(1)} \theta(u), \end{aligned} \quad (\text{A.44})$$

where

$$\mathcal{S} = -5 - \frac{4}{3} \pi^2 - 8 \ln^2 w - 4 \text{Li}_2(1-w). \quad (\text{A.45})$$

The singular terms are

$$\left\{ W_{1,\delta}^{99(1)}, W_{2,\delta}^{99(1)}, W_{3,\delta}^{99(1)} \right\} = \frac{\ln w}{1-w} \left\{ \frac{w}{2} (4-5w), 10(1-w), 4-5w \right\}, \quad (\text{A.46})$$

$$\begin{aligned} \left\{ W_{1,\delta}^{79(1)}, W_{2,\delta}^{79(1)}, W_{3,\delta}^{79(1)} \right\} = & \frac{\ln w}{(1-w)^2} \left\{ \frac{w}{2} (8-9w), -2(1-w), 8-9w \right\} \\ & - \frac{1}{1-w} \left\{ \frac{w}{2}, 0, 1 \right\} \ln \frac{\mu_b^2}{m_b^2}, \end{aligned} \quad (\text{A.47})$$

$$\begin{aligned} \left\{ W_{1,\delta}^{77(1)}, W_{2,\delta}^{77(1)}, W_{3,\delta}^{77(1)} \right\} = & \frac{8 \ln w}{(1-w)^2} \{w, -6(1-w), 2\} - \frac{2(2+w)}{(1-w)^2} \{0, 0, 1\} \\ & - \frac{2}{(1-w)^2} \{w, -4(1-w), 2\} \ln \frac{\mu_b^2}{m_b^2}. \end{aligned} \quad (\text{A.48})$$

The finite terms are

$$W_{1,\theta}^{99(1)} = \frac{\mathcal{I}}{2u\lambda} (u^4 + 4u^3 w - 8u^3 + 7u^2 w^2 - 14u^2 w + 6uw^3 - 8uw^2 + 2w^4)$$

$$+ \frac{1}{4\lambda}(u^2 + 4uw + 12u + 3w^2), \quad (\text{A.49})$$

$$W_{2,\theta}^{99(1)} = \frac{2\mathcal{I}}{u\lambda^2}(u^4w + 4u^3w^2 - 16u^3w + 12u^3 + 7u^2w^3 - 26u^2w^2 + 18u^2w + 6uw^4 - 8uw^3 + 2w^5) + \frac{1}{\lambda^2}(7u^3 + 29u^2w - 60u^2 + 43uw^2 - 82uw + 80u + 21w^3 - 38w^2), \quad (\text{A.50})$$

$$W_{3,\theta}^{99(1)} = \frac{\mathcal{I}}{u\lambda}(u^3 + 3u^2w - 6u^2 + 4uw^2 - 4uw + 2w^3) + \frac{1}{\lambda}(3u + 5w - 8), \quad (\text{A.51})$$

$$W_{1,\theta}^{79(1)} = \frac{\mathcal{I}}{u(1-w)\lambda}(2u^3w + u^3 + 6u^2w^2 - 9u^2w + 6uw^3 - 8uw^2 + 2w^4) - \frac{u(u+w-2)}{(1-w)\lambda}, \quad (\text{A.52})$$

$$W_{2,\theta}^{79(1)} = -\frac{4u\mathcal{I}}{\lambda^2}(u^2 + 2uw - u + w^2 - 3w) + \frac{2}{\lambda^2}(5u^2 + 4uw - 8u - w^2), \quad (\text{A.53})$$

$$W_{3,\theta}^{79(1)} = \frac{2\mathcal{I}}{u(1-w)\lambda}(2u^2w - 5u^2 + 4uw^2 - 4uw + 2w^3) + \frac{9u + 9w - 16}{(1-w)\lambda}, \quad (\text{A.54})$$

$$W_{1,\theta}^{77(1)} = -\frac{2\mathcal{I}}{u(1-w)^2\lambda}(u^4 + 2u^3w - 6u^3 - u^2w^2 + 4u^2w - 6uw^3 + 8uw^2 - 2w^4) + \frac{1}{(1-w)^2\lambda}(2u^3 + 4u^2w - 9u^2 + 4uw^2 + 4uw - 4u + 2w^3 - 3w^2), \quad (\text{A.55})$$

$$W_{2,\theta}^{77(1)} = -\frac{8\mathcal{I}}{u(1-w)\lambda^2}(u^4w - 2u^4 + 4u^3w^2 - 14u^3w + 14u^3 + 7u^2w^3 - 22u^2w^2 + 12u^2w + 6uw^4 - 8uw^3 + 2w^5) - \frac{12}{(1-w)\lambda^2}(3u^3 + 11u^2w - 22u^2 + 15uw^2 - 34uw + 32u + 7w^3 - 12w^2), \quad (\text{A.56})$$

$$W_{3,\theta}^{77(1)} = \frac{4\mathcal{I}}{u(1-w)^2\lambda}(u^3 + u^2w - 4u^2 + 4uw^2 - 4uw + 2w^3) - \frac{4(u-4)(u+w-2)}{(1-w)^2\lambda}. \quad (\text{A.57})$$

The results for $W_a^{99(1)}$ are identical to those presented in eqs. (2.10) and (3.18) – (3.23) of [38]. Note that the $1/u$ singularity in the last term in the square bracket of eq. (A.44) cancels against the singularities in $W_{a,\theta}^{ij(1)}$ (the last terms in the first bracket of eqs. (A.49) – (A.57)); the absence of a singularity in eq. (A.53) reflects the absence of the corresponding singular term in eq. (A.44) due to $W_{2,\delta}^{79(0)} = 0$.

Explicit results for the $O(\alpha_s\lambda_1/m_b^2)$ terms $W_a^{ij(\lambda_1,1)}$ have been obtained using reparameterization invariance relations first presented in [42] and summarized in section 5 of [38]. As a cross check of these manipulations we verified that the terms $W_a^{99(\lambda_1,1)}$ reproduce exactly the results of [38] and that the integral of the $O(\alpha_s\lambda_1/m_b^2)$ corrections over the whole hadronic spectrum amounts to an overall factor $(1 - \lambda_1/(2m_b^2))$.

B Plus distribution technology

The plus distribution of order (m, n) , for integers $m \geq 0$ and $n \geq 1$ is defined by

$$\int_{-\infty}^{\infty} du \left[\frac{\ln^m u}{u^n} \right]_+ f(u) = \int_0^1 du \frac{\ln^m u}{u^n} \left(f(u) - \sum_{k=0}^{n-1} \frac{1}{k!} f^{(k)}(0) u^k \right) \quad (\text{B.1})$$

for an arbitrary analytic function f . The simplification

$$u^k \left[\frac{\ln^m u}{u^n} \right]_+ = \begin{cases} \left[\frac{\ln^m u}{u^{n-k}} \right]_+ & k < n \\ u^{k-n} \ln^m u \theta(u) \theta(1-u) & k \geq n \end{cases} \quad (\text{B.2})$$

is consistent with the definition above, since multiplying both sides of eq. (B.2) by an analytic function and integrating over \mathbb{R} gives equality by means of eq. (B.1). Generalizing,

$$f(u) \left[\frac{\ln^m u}{u^n} \right]_+ = \sum_{k=0}^{n-1} \frac{1}{k!} f^{(k)}(0) \left[\frac{\ln^m u}{u^{n-k}} \right]_+ + \frac{\ln^m u}{u^n} \left(f(u) - \sum_{k=0}^{n-1} \frac{1}{k!} f^{(k)}(0) u^k \right) \theta(u) \theta(1-u). \quad (\text{B.3})$$

By definition, the k^{th} derivative $D^{(k)}$ of a distribution D inherits the properties of D after k applications of integration by parts. Assuming no boundary conditions at infinity,

$$\int_{-\infty}^{\infty} du D^{(k)}(u) f(u) = (-1)^k \int_{-\infty}^{\infty} du D(u) f^{(k)}(u). \quad (\text{B.4})$$

To simplify expressions of the form $f(u)D^{(k)}(u)$, we integrate by parts

$$\int_{-\infty}^{\infty} du \left[f(u) D^{(k)}(u) \right] g(u) = (-1)^k \int_{-\infty}^{\infty} du D(u) \frac{d^k}{du^k} \left[f(u) g(u) \right], \quad (\text{B.5})$$

and then work (on a case by case basis) to remove the derivatives of $g(u)$ by integrating by parts again, so that $g(u)$ is restored and factors out of the integral. For instance,

$$\begin{aligned} \int_{-\infty}^{\infty} du \left[f(u) \delta'(u) \right] g(u) &= - \int_{-\infty}^{\infty} du \delta(u) \left[f(0) g'(u) + f'(0) g(u) \right] \\ &= \int_{-\infty}^{\infty} du \left[f(0) \delta'(u) - f'(0) \delta(u) \right] g(u), \end{aligned} \quad (\text{B.6})$$

so $f(u)\delta'(u) = f(0)\delta'(u) - f'(0)\delta(u)$, which generalizes for higher derivatives to

$$f(u)\delta^{(n)}(u) = \sum_{k=0}^n (-1)^k \binom{n}{k} f^{(k)}(0) \delta^{(n-k)}(u). \quad (\text{B.7})$$

The derivative of a plus distribution is given in terms of higher order plus distributions and singular distributions,

$$\frac{d}{du} \left[\frac{\ln^m u}{u^n} \right]_+ = \begin{cases} -n \left[\frac{1}{u^{n+1}} \right]_+ + \sum_{k=0}^n \frac{(-1)^k}{k!} \delta^{(k)}(u) - \delta(1-u) & m = 0 \\ -n \left[\frac{\ln^m u}{u^{n+1}} \right]_+ + m \left[\frac{\ln^{m-1} u}{u^{n+1}} \right]_+ & m > 0. \end{cases} \quad (\text{B.8})$$

For instance,

$$\begin{aligned}
\int_{-\infty}^{\infty} \frac{d}{du} \left[\frac{1}{u} \right]_+ f(u) du &= - \int_{-\infty}^{\infty} \left[\frac{1}{u} \right]_+ f'(u) du = - \int_0^1 \frac{f'(u) - f'(0)}{u} du \\
&= - \int_0^1 \frac{f(u) - f(0) - uf'(0)}{u^2} du - \frac{f(u) - f(0) - uf'(0)}{u} \Big|_0^1 \\
&= \int_{-\infty}^{\infty} \left(- \left[\frac{1}{u^2} \right]_+ + \delta(u) - \delta'(u) - \delta(1-u) \right) f(u) du.
\end{aligned} \tag{B.9}$$

When the derivative of a plus distribution comes multiplied by an analytic function, the derivative is eliminated according to eq. (B.8), and then eqs. (B.3) and (B.7) are used to further reduce the result to a standard form in which the coefficients of the plus distributions and Dirac distributions are independent of u . Moreover, second and higher order derivatives are obtained simply by iterating eq. (B.8). Finally, derivatives of finite distributions generate singular distributions from their logarithmic singularities,

$$\frac{d}{du} \left[\ln^m u \theta(u) \theta(1-u) \right] = m \left[\frac{\ln^{m-1} u}{u} \right]_+. \tag{B.10}$$

For instance,

$$\begin{aligned}
\int_{-\infty}^{\infty} \frac{d}{du} \left[\ln u \theta(u) \theta(1-u) \right] f(u) du &= - \int_{-\infty}^{\infty} \left[\ln u \theta(u) \theta(1-u) \right] f'(u) du \\
&= - \int_0^1 \ln u f'(u) du = \int_0^1 \frac{f(u) - f(0)}{u} du + \ln u \left(f(u) - f(0) \right) \Big|_0^1 \\
&= \int_{-\infty}^{\infty} \left[\frac{1}{u} \right]_+ f(u) du.
\end{aligned} \tag{B.11}$$

References

- [1] T. Hurth and M. Nakao, *Radiative and Electroweak Penguin Decays of B Mesons*, *Ann. Rev. Nucl. Part. Sci.* **60** (2010) 645–677, [[1005.1224](#)].
- [2] T. Hurth, *Present status of inclusive rare B decays*, *Rev. Mod. Phys.* **75** (2003) 1159–1199, [[hep-ph/0212304](#)].
- [3] LHCb collaboration, R. Aaij et al., *Angular Analysis of the $B^+ \rightarrow K^{*+} \mu^+ \mu^-$ Decay*, *Phys. Rev. Lett.* **126** (2021) 161802, [[2012.13241](#)].
- [4] LHCb collaboration, R. Aaij et al., *Measurement of CP-Averaged Observables in the $B^0 \rightarrow K^{*0} \mu^+ \mu^-$ Decay*, *Phys. Rev. Lett.* **125** (2020) 011802, [[2003.04831](#)].
- [5] LHCb collaboration, R. Aaij et al., *Differential branching fraction and angular moments analysis of the decay $B^0 \rightarrow K^+ \pi^- \mu^+ \mu^-$ in the $K_{0,2}^*(1430)^0$ region*, *JHEP* **12** (2016) 065, [[1609.04736](#)].
- [6] LHCb collaboration, R. Aaij et al., *Measurements of the S-wave fraction in $B^0 \rightarrow K^+ \pi^- \mu^+ \mu^-$ decays and the $B^0 \rightarrow K^{*}(892)^0 \mu^+ \mu^-$ differential branching fraction*, *JHEP* **11** (2016) 047, [[1606.04731](#)].

- [7] LHCb collaboration, R. Aaij et al., *Angular analysis of the $B^0 \rightarrow K^{*0} \mu^+ \mu^-$ decay using 3 fb^{-1} of integrated luminosity*, *JHEP* **02** (2016) 104, [[1512.04442](#)].
- [8] LHCb collaboration, R. Aaij et al., *Angular analysis of the rare decay $B_s^0 \rightarrow \phi \mu^+ \mu^-$* , *JHEP* **11** (2021) 043, [[2107.13428](#)].
- [9] LHCb collaboration, R. Aaij et al., *Branching Fraction Measurements of the Rare $B_s^0 \rightarrow \phi \mu^+ \mu^-$ and $B_s^0 \rightarrow f_2'(1525) \mu^+ \mu^-$ Decays*, *Phys. Rev. Lett.* **127** (2021) 151801, [[2105.14007](#)].
- [10] LHCb collaboration, R. Aaij et al., *Angular analysis and differential branching fraction of the decay $B_s^0 \rightarrow \phi \mu^+ \mu^-$* , *JHEP* **09** (2015) 179, [[1506.08777](#)].
- [11] LHCb collaboration, R. Aaij et al., *Angular moments of the decay $\Lambda_b^0 \rightarrow \Lambda \mu^+ \mu^-$ at low hadronic recoil*, *JHEP* **09** (2018) 146, [[1808.00264](#)].
- [12] LHCb collaboration, R. Aaij et al., *Differential branching fraction and angular analysis of $\Lambda_b^0 \rightarrow \Lambda \mu^+ \mu^-$ decays*, *JHEP* **06** (2015) 115, [[1503.07138](#)].
- [13] N. Gubernari, M. Reboud, D. van Dyk and J. Virto, *Improved theory predictions and global analysis of exclusive $b \rightarrow s \mu^+ \mu^-$ processes*, *JHEP* **09** (2022) 133, [[2206.03797](#)].
- [14] T. Hurth, F. Mahmoudi, D. Martinez Santos and S. Neshatpour, *Neutral current B-decay anomalies*, in *8th Workshop on Theory, Phenomenology and Experiments in Flavour Physics: Neutrinos, Flavor Physics and Beyond*, 10, 2022. [[2210.07221](#)].
- [15] T. Hurth, F. Mahmoudi and S. Neshatpour, *Model independent analysis of the angular observables in $B^0 \rightarrow K^{*0} \mu^+ \mu^-$ and $B^+ \rightarrow K^{*+} \mu^+ \mu^-$* , *Phys. Rev. D* **103** (2021) 095020, [[2012.12207](#)].
- [16] M. Bordone, G. Isidori and A. Pattori, *On the Standard Model predictions for R_K and R_{K^*}* , *Eur. Phys. J. C* **76** (2016) 440, [[1605.07633](#)].
- [17] LHCb collaboration, R. Aaij et al., *Test of lepton universality with $B^0 \rightarrow K^{*0} \ell^+ \ell^-$ decays*, *JHEP* **08** (2017) 055, [[1705.05802](#)].
- [18] LHCb collaboration, R. Aaij et al., *Test of lepton universality in beauty-quark decays*, *Nature Phys.* **18** (2022) 277–282, [[2103.11769](#)].
- [19] T. Hurth, F. Mahmoudi, D. M. Santos and S. Neshatpour, *More Indications for Lepton Nonuniversality in $b \rightarrow s \ell^+ \ell^-$* , *Phys. Lett. B* **824** (2022) 136838, [[2104.10058](#)].
- [20] LHCb collaboration, *Measurement of lepton universality parameters in $B^+ \rightarrow K^+ \ell^+ \ell^-$ and $B^0 \rightarrow K^{*0} \ell^+ \ell^-$ decays*, [[2212.09153](#)].
- [21] T. Huber, T. Hurth, J. Jenkins, E. Lunghi, Q. Qin and K. K. Vos, *Phenomenology of inclusive $\bar{B} \rightarrow X_s \ell^+ \ell^-$ for the Belle II era*, *JHEP* **10** (2020) 088, [[2007.04191](#)].
- [22] T. Hurth, M. Fickinger, S. Turczyk and M. Benzke, *Resolved Power Corrections to the Inclusive Decay $\bar{B} \rightarrow X_s \ell^+ \ell^-$* , *Nucl. Part. Phys. Proc.* **285-286** (2017) 57–62, [[1711.01162](#)].
- [23] M. Benzke, T. Hurth and S. Turczyk, *Subleading power factorization in $\bar{B} \rightarrow X_s \ell^+ \ell^-$* , *JHEP* **10** (2017) 031, [[1705.10366](#)].
- [24] M. Benzke and T. Hurth, *Resolved $1/m_b$ contributions to $b \rightarrow s \ell \ell$ and $b \rightarrow s \gamma$* , [[2006.00624](#)].
- [25] BELLE-II collaboration, W. Altmannshofer et al., *The Belle II Physics Book*, *PTEP* **2019** (2019) 123C01, [[1808.10567](#)].

- [26] Y. Amhis and P. Owen, *Isospin extrapolation as a method to study inclusive $\bar{B} \rightarrow X_s \ell^+ \ell^-$ decays*, *Eur. Phys. J. C* **82** (2022) 371, [[2106.15943](#)].
- [27] BABAR collaboration, B. Aubert et al., *Measurement of the $B \rightarrow X_s \ell^+ \ell^-$ branching fraction with a sum over exclusive modes*, *Phys. Rev. Lett.* **93** (2004) 081802, [[hep-ex/0404006](#)].
- [28] BABAR collaboration, J. P. Lees et al., *Measurement of the $B \rightarrow X_s \ell^+ \ell^-$ branching fraction and search for direct CP violation from a sum of exclusive final states*, *Phys. Rev. Lett.* **112** (2014) 211802, [[1312.5364](#)].
- [29] BELLE collaboration, M. Iwasaki et al., *Improved measurement of the electroweak penguin process $B \rightarrow X_s \ell^+ \ell^-$* , *Phys. Rev. D* **72** (2005) 092005, [[hep-ex/0503044](#)].
- [30] BELLE collaboration, Y. Sato et al., *Measurement of the lepton forward-backward asymmetry in $B \rightarrow X_s \ell^+ \ell^-$ decays with a sum of exclusive modes*, *Phys. Rev. D* **93** (2016) 032008, [[1402.7134](#)].
- [31] A. Ali and G. Hiller, *Perturbative QCD corrected and power corrected hadron spectra and spectral moments in the decay $B \rightarrow X_s \ell^+ \ell^-$* , *Phys. Rev. D* **58** (1998) 074001, [[hep-ph/9803428](#)].
- [32] M. Neubert, *Analysis of the photon spectrum in inclusive $B \rightarrow X_s \gamma$ decays*, *Phys. Rev. D* **49** (1994) 4623–4633, [[hep-ph/9312311](#)].
- [33] SIMBA collaboration, F. U. Bernlochner, H. Lacker, Z. Ligeti, I. W. Stewart, F. J. Tackmann and K. Tackmann, *Precision Global Determination of the $B \rightarrow X_s \gamma$ Decay Rate*, *Phys. Rev. Lett.* **127** (2021) 102001, [[2007.04320](#)].
- [34] K. S. M. Lee, Z. Ligeti, I. W. Stewart and F. J. Tackmann, *Universality and m_X cut effects in $B \rightarrow X_s \ell^+ \ell^-$* , *Phys. Rev. D* **74** (2006) 011501, [[hep-ph/0512191](#)].
- [35] G. Bell, M. Beneke, T. Huber and X.-Q. Li, *Heavy-to-light currents at NNLO in SCET and semi-inclusive $\bar{B} \rightarrow X_s \ell^+ \ell^-$ decay*, *Nucl. Phys. B* **843** (2011) 143–176, [[1007.3758](#)].
- [36] K. S. M. Lee and F. J. Tackmann, *Nonperturbative m_X cut effects in $B \rightarrow X_s \ell^+ \ell^-$ observables*, *Phys. Rev. D* **79** (2009) 114021, [[0812.0001](#)].
- [37] A. Gunawardana and G. Paz, *Reevaluating uncertainties in $\bar{B} \rightarrow X_s \gamma$ decay*, *JHEP* **11** (2019) 141, [[1908.02812](#)].
- [38] B. Capdevila, P. Gambino and S. Nandi, *Perturbative corrections to power suppressed effects in $\bar{B} \rightarrow X_u \ell \nu$* , *JHEP* **04** (2021) 137, [[2102.03343](#)].
- [39] K. S. M. Lee, Z. Ligeti, I. W. Stewart and F. J. Tackmann, *Extracting short distance information from $b \rightarrow s \ell^+ \ell^-$ effectively*, *Phys. Rev. D* **75** (2007) 034016, [[hep-ph/0612156](#)].
- [40] T. Huber, T. Hurth and E. Lunghi, *Inclusive $\bar{B} \rightarrow X_s \ell^+ \ell^-$: complete angular analysis and a thorough study of collinear photons*, *JHEP* **06** (2015) 176, [[1503.04849](#)].
- [41] T. Huber, E. Lunghi, M. Misiak and D. Wyler, *Electromagnetic logarithms in $\bar{B} \rightarrow X_s \ell^+ \ell^-$* , *Nucl. Phys. B* **740** (2006) 105–137, [[hep-ph/0512066](#)].
- [42] A. V. Manohar, *Reparametrization Invariance Constraints on Inclusive Decay Spectra and Masses*, *Phys. Rev. D* **82** (2010) 014009, [[1005.1952](#)].
- [43] P. Gambino, K. J. Healey and S. Turczyk, *Taming the higher power corrections in semileptonic B decays*, *Phys. Lett. B* **763** (2016) 60–65, [[1606.06174](#)].

- [44] T. Huber, T. Hurth, J. Jenkins, E. Lunghi, Q. Qin and K. K. Vos, *Long distance effects in inclusive rare B decays and phenomenology of $\bar{B} \rightarrow X_d \ell^+ \ell^-$* , *JHEP* **10** (2019) 228, [[1908.07507](#)].
- [45] PARTICLE DATA GROUP collaboration, R. L. Workman et al., *Review of Particle Physics*, *PTEP* **2022** (2022) 083C01.
- [46] Z.-z. Xing, H. Zhang and S. Zhou, *Updated Values of Running Quark and Lepton Masses*, *Phys. Rev. D* **77** (2008) 113016, [[0712.1419](#)].
- [47] Z. Ligeti and F. J. Tackmann, *Precise predictions for $B \rightarrow X_s \ell^+ \ell^-$ in the large q^2 region*, *Phys. Lett. B* **653** (2007) 404–410, [[0707.1694](#)].
- [48] V. Shtabovenko, R. Mertig and F. Orellana, *FeynCalc 9.3: New features and improvements*, *Comput. Phys. Commun.* **256** (2020) 107478, [[2001.04407](#)].
- [49] A. V. Smirnov, *Algorithm FIRE – Feynman Integral REduction*, *JHEP* **10** (2008) 107, [[0807.3243](#)].
- [50] M. Czakon, *Automatized analytic continuation of Mellin-Barnes integrals*, *Comput. Phys. Commun.* **175** (2006) 559–571, [[hep-ph/0511200](#)].
- [51] M. Czakon, <http://mbtools.hepforge.org/>, .